was demonstrated by minimal histone acetylation in HeLa cells. ChIP-chip also demonstrated interactions of the erythroid-specific transcription factor GATA-1 with several sites in the *HBS1L-MYB* interval. GATA-1 signals in coincidence with the DNase I hypersensitive sites in *HMIP* block 2 strongly suggest the presence of regulatory elements. Regulatory activity of the intergenic region was validated by presence of intergenic transcripts in erythroid precursor cells in a tiling microarray. We postulate that the regulatory elements distally control *MYB* expression, which in turn influences erythroid differentiation and, indirectly, the control of HbF levels.

The use of microarrays also allowed us to compare patterns of activity in the candidate interval with other regions encompassing widely expressed genes across 70 Mb of chromosome 6q. We further provide a large-scale analysis of GATA-1 occupancy in erythroid cells that includes the entire β and α globin gene clusters.

Methods

Cells and cell cultures

Cell lines were maintained in RPMI-1620 medium (Sigma-Aldrich) with the addition of 10% of fetal calf serum (FCS; PAA-laboratories), 2 mM L-glutamine (Sigma-Aldrich), 0.1 mg/mL streptomycin, and 18 units/mL penicillin (Sigma-Aldrich). Concentrations were kept at 0.5 to 1.0 × 10^6 cells/mL. K562 cells were treated with 40 μM hemin (Sigma-Aldrich) for 24 hours to induce differentiation.

Primary human erythroid cells were cultured from peripheral blood using a 2-phase liquid system as previously described.[11,17] Cytospins of erythroid progenitors from different days of culture were stained using a Giemsa staining set (Hema "Gurr"; VWR) according to the manufacturer's protocol.

Flow cytometry of primary erythroid cells was performed with anti–human CD71 monoclonal antibodies (FITC conjugated, 555536; BD Biosciences) or anti–human glycophorin A (GPA, phycoerythrin [PE] conjugated, R7078; DAKO) as previously described.[11]

DNase I hypersensitivity analyses

DNase I hypersensitivity analysis of *HMIP-2* was performed on 2 biologic replicates of induced and uninduced K562 cells, and Jurkat cells. Nuclei were treated with 70 units of DNase I at 37°C for 3 minutes as determined by optimization experiments (supplemental methods and supplemental Figure 1, available on the *Blood* website; see the Supplemental Materials link at the top of the online article). Real-time quantitative polymerase chain reaction (PCR)[18,19] was performed in triplicate on 20 ng DNA samples using SYBR Green PCR Mastermix (Applied Biosystems) and the ABI Prism 7900HT Sequence Detection system (Applied Biosystems).

The *HMIP-2* region could be covered in 68 overlapping fragments of approximately 500 bp (PCR primer sequences available on request). Relative sensitivity to DNase I for each target was calculated by converting delta C_T (difference in C_T values between treated and untreated DNAs) to a linear scale and plotted as a function of primer position. Values were normalized to the negative control *NEFM* (supplemental methods and supplemental Figure 1) to account for differences in treatment conditions.

Chromatin immunoprecipitation

Antibodies used for ChIP experiments included anti-diacetylated histone H3 (K9 and 14; no. 06-599; Millipore), anti–tetra-acetylated histone H4 (K5, 8, 12, and 16; no. 06-866; Millipore), anti-RNA polymerase II (no. 05-623; Millipore), and anti–GATA-1 (no. sc-1234; Santa Cruz Biotechnology).

ChIP experiments for acetylated histones were performed using the EZ-ChIP protein G kit (no. 17-371; Millipore) according to the manufacturer's protocol with minor modifications (Dr David Garrick, Weatherall Institute of Molecular Medicine, Oxford, United Kingdom). ChIP for RNA polymerase II and GATA-1 was performed using the Magna ChIP protein G kit (no. 17-611; Millipore) according to the manufacturer's protocol with minor modifications.

ChIP assays were performed on cultured primary human erythroid cells (phase II, day 10) and HeLa cells. Cells (5 × 10^7 per experiment) were cross-linked in 10 mL growth medium with 1% formaldehyde (Sigma-Aldrich) for 10 minutes at room temperature, and the chromatin was sonicated (10 × 15 seconds, Sonic VibraCell at 40% efficiency) to a size of approximately 500 base pairs (bp; range 200-1000 bp). Immunoprecipitations were performed after an overnight incubation with 5 to 10 μg of the appropriate antibody, with protein G agarose beads, or with protein G magnetic beads. A sample containing no antibody was used as a negative control.

ChIP material was validated by SYBR Green quantitative PCR before microarray analyses using different positive control targets. Enrichment of a specific target sequence in ChIP material was calculated relative to input DNA, and the results were normalized to a control sequence in exon 1 of the neurofilament gene *(NEFM)* representing an inactive gene (data not shown).

Microarray analysis of ChIP material

Two microarrays, both from Roche-NimbleGen, were used in these experiments as described in the supplemental methods. The first array encompassed 70 Mb (positions 93 424 310 to 165 905 673; hg18) on chromosome 6, including the 6q23 HbF locus. The second was a custom array and included the globin loci as controls. The microarray data have been deposited with Gene Expression Omnibus (GEO) under accession number GSE16541.[20]

Input and ChIP DNA were amplified using a whole genome amplification kit (WGA1; Sigma-Aldrich) applying a previously described protocol adapted for ChIP material.[21] Amplified DNA was purified using a QIAquick PCR purification kit (QIAGEN) with buffer PBI substituted for buffer PB.

Arrays were hybridized and washed using Roche-NimbleGen kits according to the manufacturer's protocol. Scanning was performed using a GenePix 4000B Scanner (Molecular Devices). Detailed protocol, including data extraction and analysis, is shown in supplemental methods.

Transcript Tiling Array

A customized Affymetrix GeneChip Tiling Array was designed to identify novel transcripts[22] between positions 135 323 209 and 135 582 003 (NCBI build 36[23]) that encompass the entire *MYB* and *HBS1L* genes as well as the intergenic region; 116 858 bases containing human repetitive sequence were excluded from probe design. The remaining 141 937 bases were tiled by overlapping oligonucleotides. The starting position of each 25mer oligo was shifted by 2 bases within *HBS1L* and *MYB*, and by one base within the intergenic region. Oligonucleotides were designed for both DNA strands. A total of 224 258 oligonucleotide probes was included in each array.

Total RNA was extracted from erythroid cells (liquid culture phase II, days 3 and 5)[11,17] using Tri-Reagent (Sigma-Aldrich). Five micrograms was treated with the RiboMinus Transcriptome Isolation Kit (Invitrogen) to remove ribosomal RNA before cDNA synthesis according to the manufacturer's instructions. Synthesis of cDNA, fragmentation, and end labeling was performed using the GeneChip Whole Transcript Double-Stranded Target Assay kit (Affymetrix) according to the manufacturer's instructions. After hybridization for 16 hours, the arrays were washed and stained using a Fluidics Station 450 (Affymetrix). Scanning was performed by GeneChip Scanner 3000 7G (Affymetrix). Data analysis was performed using Affymetrix Tiling Analysis Software Version 1.1 and data were visualized using the Affymetrix Integrated Genome Browser. Because double-stranded cDNA was used, the transcript maps correspond to the signals from both strands.

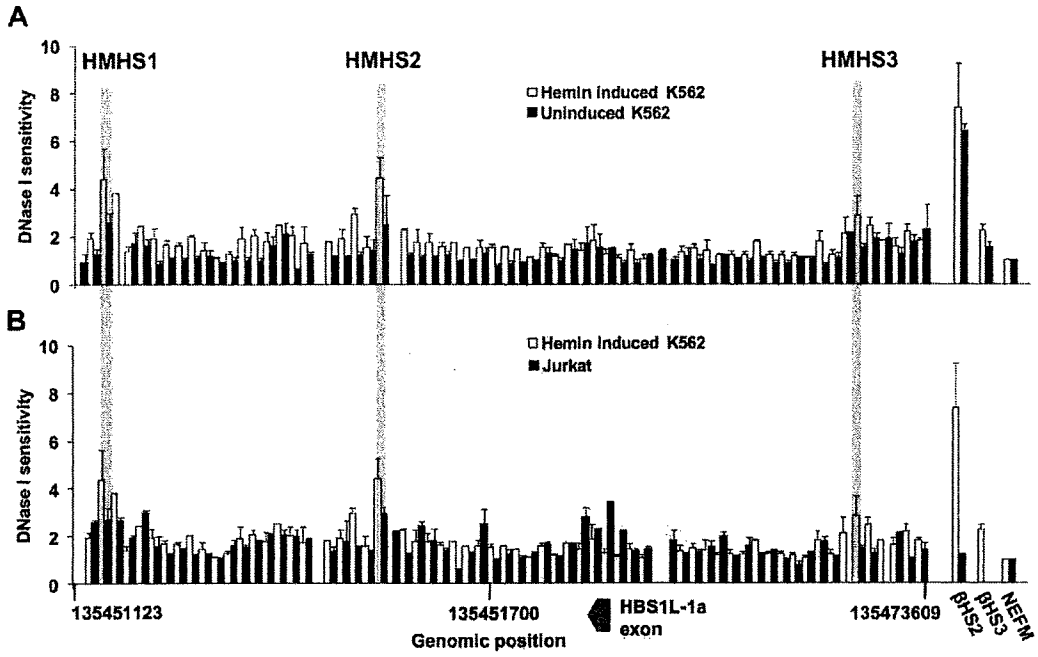

Figure 1. DNase I digestion profiles of the *HBS1L-MYB* intergenic region in *HMIP* block 2. DNase I sensitivity was analyzed by real-time PCR using 68 primer pairs spanning the 24-kb *HMIP-2* region. Control primers targeting the β-globin LCR HS2 and HS3 (βHS2 and βHS3) and the *NEFM* gene were also included in experiments. Relative sensitivity to DNase I for each target was calculated from delta C_T values between treated and untreated samples and normalized to *NEFM*. DNase I sensitivity was plotted as a function of primer position. Error bars represent differences between 2 biologic repeats. (A) DNase I sensitivity in *HMIP-2* compared between hemin-induced and uninduced K562 cells. Three DNase I hypersensitive sites (HMHS1, HMHS2, and HMHS3; gray bars) were identified in hemin-induced K562 cells. (B) DNase I sensitivity in *HMIP-2* compared between hemin-induced K562 cells and Jurkat cells. The 3 hypersensitive sites in hemin-induced K562 cells showed no or less sensitivity to DNase I in Jurkat cells. Hypersensitivity was instead observed in Jurkat cells at the site of the *HBS1L-1a* exon, which showed no hypersensitivity in K562 cells (induced and uninduced). The βHS3 control was not included for DNase I sensitivity analyses in Jurkat cells.

Results

HBS1L-MYB intergenic region is sensitive to DNase I in erythroid cells

Variants in block 2 of the *HBS1L-MYB* intergenic region account for the majority of the genetic association with HbF in the 6q QTL region. We performed DNase I hypersensitivity analysis along the entire 24 kb of *HMIP-2* in K562 cells as a screen for genetic regulatory elements. K562 cells treated with hemin were induced to differentiate, resulting in strong up-regulation of globin gene expression and simultaneous down-regulation of *MYB* expression.[24,25] After 24 hours of hemin treatment (at 40 μM), β globin expression increased 9.5-fold, that of γ globin, 5-fold, whereas *MYB* expression decreased by 7-fold (data not shown). DNase I hypersensitivity profiles were studied in uninduced and hemin-induced K562 cells, and in Jurkat cells (T-cell leukemia), representing a nonerythroid cell line. Two biologic repeats were performed for each cell type. Analysis of both βHS2 and βHS3 (positive controls) and *NEFM* (negative control) were included for K562 cells and βHS2 and *NEFM*, for Jurkat cells.

In uninduced K562 cells, several sites within *HMIP-2* showed sensitivity to DNase I above background levels, indicating an open chromatin structure (Figure 1A). When cells were induced to differentiate, the region showed a general increase in DNase I sensitivity; 3 sites referred to here as *HBS1L-MYB* (HM) HS1, HS2, and HS3, in particular, showed a marked increase in sensitivity compared with background levels (Figure 1A). DNase I sensitivity also increased for βHS2 and βHS3 controls, consistent with the induction in globin gene expression. HMHS1, HMHS2, and HMHS3 also showed stronger sensitivity to DNase I than the βHS3 control, thereby reaching a threshold level for hypersensitivity (Figure 1A). There was no difference in DNase I sensitivity for *NEFM* in uninduced and induced K562 cells.

As expected, βHS2 was not sensitive to DNase I in Jurkat cells, a nonerythroid cell line (Figure 1B). In the *HMIP* block 2 region, Jurkat cells show similar background levels and generally, a similar DNase I sensitivity profile to induced K562 cells, but with much less sensitivity at HMHS1, HMHS2, and HMHS3, indicating that DNase I sensitivity at these sites is tissue specific (Figure 1B). The strongest sensitivity to DNase I in Jurkat cells coincided with the putative promoter region of the alternative *HBS1L* exon (exon 1a), which showed a low degree of sensitivity in K562 cells (both uninduced and induced). This is consistent with expression of the *HBS1L-1a* transcript in Jurkat cells but not in K562 cells.[8] To validate the promoter prediction at *HBS1L-1a*, we examined its functional property in a reporter assay; the region showed activity in Jurkat cells but not in K562 cells (supplemental Figure 2). The *HBS1L* exon *1a* promoter therefore served as a positive internal control for DNase I hypersensitivity at an active regulatory element within the *HMIP* block 2 region.

Characterization of erythroid and nonerythroid cells for use in chromatin immunoprecipitation

The identification of DNase I hypersensitive sites in *HMIP* block 2 in hemin-induced K562 cells suggested that the intergenic region contained regulatory elements active in erythroid lineages and encouraged further functional analysis of the interval. We assessed the chromatin activity and transcription factor binding throughout the *HBS1L-MYB* and flanking regions of chromosome 6q, and tissue-specific activity of these profiles. Primary human erythroid progenitors cultured in a 2-phase liquid system were analyzed to

select optimum time of harvest when *HBS1L, MYB,* and the globin genes were fully expressed. HeLa cells served as examples of a *MYB*-negative cell line.

Basophilic erythroblasts from phase II, day 10, were chosen for ChIP analysis (supplemental methods and supplemental Figure 3). At this stage, expression profiles indicated that the cells were in a state of high transcriptional activity; the candidate genes *(HBS1L* and *MYB)* as well as *GATA1* and the globin genes were expressed at high levels (data not shown).

To investigate tissue specificity of activity in the intergenic region and the relation between activity and candidate gene expression, we compared histone acetylation patterns in the intergenic region between erythroid precursor cells and a cell line lacking *HBS1L* and *MYB* expression. Eight cell lines, which included Jurkat, HL60 (promyelocytic leukemia), U937 (monocytic leukemia), HeLa (cervical cancer), HEK293 (kidney), HuH-7 (liver carcinoma), U2OS (osteosarcoma), and HKC-8 (renal epithelial), were screened, together with K562 cells and primary erythroid cells for *HBS1L* and *MYB* expression using TaqMan reverse transcription PCR. *HBS1L* was highly expressed in all lines analyzed (real-time PCR C_T values of 23-26), which indicates a housekeeping function (supplemental Figure 4A). In contrast, *MYB* expression varied dramatically; it was highly expressed in all hematopoietic cell–related lines (C_T values of 24-26) but minimally expressed in other lines (C_T values of 31-35; supplemental Figure 4B). HeLa, which showed relatively low *HBS1L* expression (10% of expression in erythroid precursors) and insignificant *MYB* expression (0.01% of expression observed in erythroid precursors), was chosen to represent a *MYB*-negative cell line in ChIP experiments.

Overview of histone acetylation, GATA-1, and RNA polymerase II interactions across chromosome 6q

On viewing the ChIP-chip data from erythroid precursors across 70 Mb of chromosome 6q represented on the array, it was evident that all antibodies showed similar patterns of activity. The strongest peaks were found in gene-rich areas, whereas large intergenic sequences lacked signal (supplemental Figure 5). Well-defined areas of high levels of AcH3 were seen at transcriptional start sites (TSSs) with a less defined pattern for AcH4 as previously described.[26] Interestingly, abundant GATA-1 signals were found over the entire 70-Mb region in coincidence with RNAP II signals at active genes. The gene-free *HBS1L-MYB* interval showed strong signals for all antibodies in erythroid cells, indicating a high level of activity in this region.

Publicly available expression data from the UCSC Genome Browser (http://genome.ucsc.edu)[27] revealed that a majority of the genes that showed strong signals for histone acetylation, RNAP II, and GATA-1 were hematopoietic specific, but a few ubiquitous genes were also included. The genes represented a wide range of functions including transcription factors, adhesion receptors, and signaling proteins, reflecting a broad target repertoire for GATA-1 as a transcription factor (supplemental Table 1).

The *HBS1L-MYB* intergenic region is highly active in erythroid precursors

ChIP-chip data of GATA-1, AcH3, AcH4, and RNAP II in erythroid precursors and AcH3 in HeLa cells was analyzed across a 2.5-Mb region of the 6q23 HbF locus, encompassing the 5 protein coding genes (including the *HBS1L-MYB* intergenic region), and flanking sequences (Figure 2). Biologic ChIP-chip replicates using primary human erythroblasts (phase II day 10 of culture) from 2 individuals provided very similar profiles.

Histone acetylation patterns and RNAP II signal in the 6q23 locus in erythroid precursors were consistent with previous expression analysis of genes in the locus[11] (Figure 2). The *PDE7B* and *ALDH8A1* genes are not expressed in erythroid precursors and consistently showed no signal of acetylation or RNAP II interaction. *AHI1* that is expressed at low levels showed some histone acetylation signal at the promoter regions. In contrast, the highly expressed *HBS1L* and *MYB* genes were associated with strong RNAP II signal and histone acetylation around the promoter regions as well as coding regions. The RNAP II antibody used detects both nonphosphorylated inactive RNAP II as well as phosphorylated actively elongating forms. Interestingly, although *MYB* is the most highly expressed gene in the region, we see no RNAPII interaction at the immediate promoter-proximal 5′ end, but instead, high levels in the body of the gene and a large accumulation toward the 3′ end and beyond (Figures 2-3). We speculate that the lack of RNAPII at the promoter is a result of rapid transcription leaving no inactive RNAPII stalling at the initiation complex. The phenomenon of RNAPII accumulation at the 3′ end of actively transcribed genes has previously been observed and is likely to reflect pausing and dephosphorylation of the polymerase before release.[28] With nonexpressed genes, RNAP II was often seen as a strong signal but only at the 5′ preinitiation complex. Strikingly, the AcH3 and AcH4 signals were equally strong in the *HBS1L-MYB* intergenic region as around the *HBS1L* and *MYB* promoters and exons, indicating that this region is highly active in erythroid precursors. In the context of the whole of 6q region analyzed, there was little evidence of such high intergenic activity elsewhere.

In contrast to the strong signals observed in erythroid cells, HeLa cells showed minimal histone acetylation, consistent with the low/absent candidate gene expression in these cells.

GATA-1 signal in the 6q23 locus was concentrated around the *MYB* and *HBS1L* area, with the strongest peaks in the core intergenic region. In fact, the GATA-1 signal in the *HBS1L-MYB* intergenic region represented the most significant GATA-1 peaks in the entire 70-Mb region covered on the 6q array.

The *HMIP-2* and *-3* regions show characteristics of a distal regulatory region in erythroid precursors

A closer view of the *HBS1L-MYB* intergenic region revealed that the histone H3 and H4 acetylation in erythroid precursor cells was found in a defined 65-kb interval encompassing the *HMIP-2* and *-3* regions (Figure 3). Within this interval, the strongest AcH3 and GATA-1 signals were concentrated in the *HMIP-2* region. The intergenic region included 7 peaks of GATA-1 signal, 3 of which were within *HMIP-2* and 1 was in *HMIP-3*. The GATA-1 signals in the *HMIP-2* region all coincided with DNase I hypersensitive sites identified in induced K562 cells as a further indication of these sites being functional regulatory elements. In addition to a GATA-1 signal approximately 7 kb 5′ of *MYB*, strong signals were seen in intron 5 of *MYB* (just upstream of exon 6) and in intron 8 (just upstream of exon 9). No GATA-1 signal, however, was detected at the immediate *MYB* promoter. GATA-1 signal was also observed at the *HBS1L* promoter region. There was a prominent coincidence of GATA-1 signal on the array with conserved GATA-1 motifs (human/mouse/rat alignment available from the UCSC Genome Browser; http://genome.ucsc.edu),[27] which support a functional relevance of these sites. Some weak RNAP II signals were also

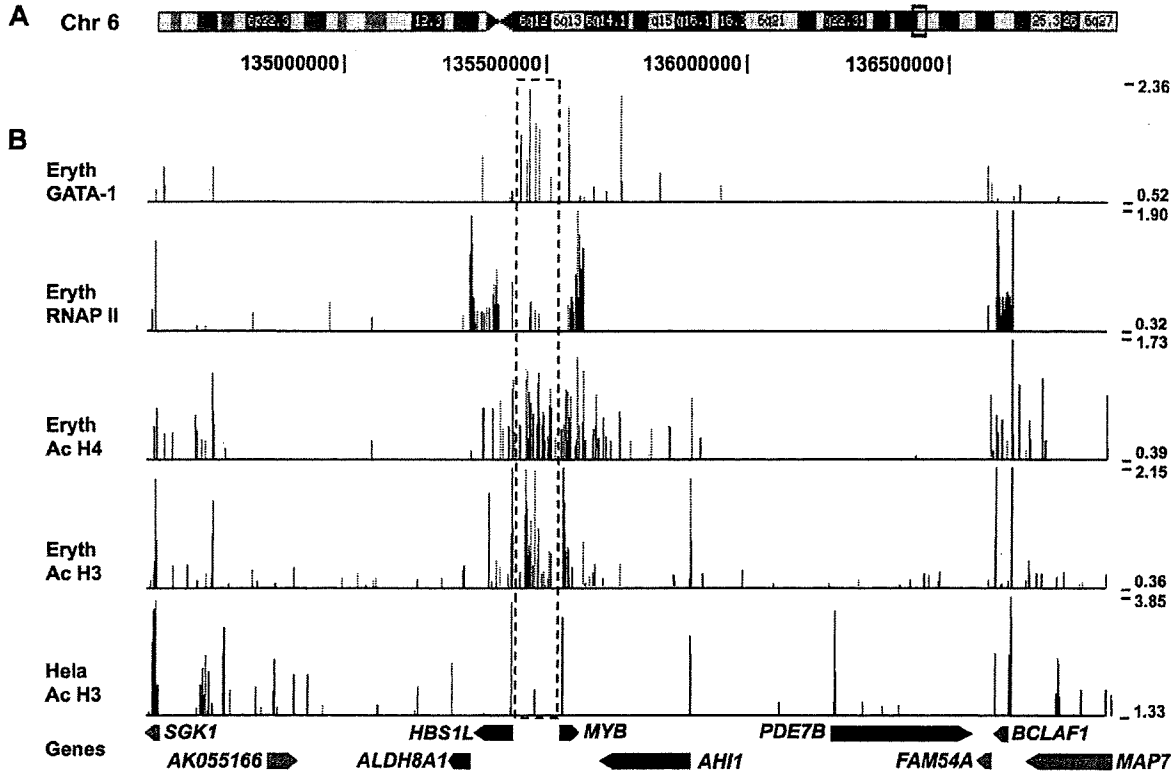

Figure 2. ChIP-chip data for the 6q23 locus in erythroid precursor and HeLa cells. (A) The box on chromosome 6 represent a 2.5-Mb region (position chr6: 134 503 000-136 928 000), which is covered in this figure and includes the 6q23 locus. (B) Results from ChIP-chip experiments for GATA-1, RNAP II, AcH4, and AcH3 in erythroid precursors and AcH3 in HeLa cells. Genes in the 6q23 locus are shown below as black arrows and other genes in gray. The *HBS1L-MYB* intergenic region is indicated by the boxed area marked with dashed lines to highlight the strong histone acetylation and GATA-1 binding signals in erythroid precursor cells. Data are displayed in the UCSC Genome Browser[27] using autoscale settings.

observed in the *HMIP-2* and *-3* regions and in coincidence with GATA-1 signal.

In contrast to the strong signals observed in erythroid precursors, histone H3 acetylation was absent in the intergenic region in HeLa cells with the exception of a restricted but significant peak in the *HMIP-2* region, coincident with HMHS3 in K562 cells and a strong GATA-1 signal in erythroid precursors. This peak is in the vicinity of the putative promoter region of *HBS1L* exon 1a.

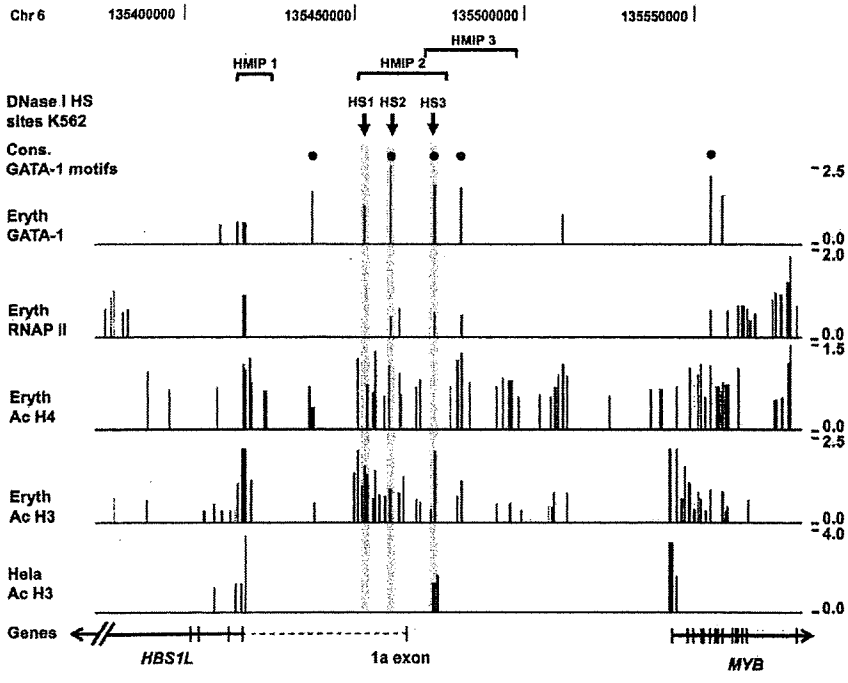

Figure 3. ChIP-chip data for the *HBS1L-MYB* intergenic region. Results from ChIP-chip experiments for GATA-1, RNAP II, AcH4, and AcH3 in erythroid precursors and AcH3 in HeLa cells. The figure covers a 210-kb region (position chr6: 135 373 000-135 582 000) and includes a part of the *HBS1L* gene, the intergenic region, and the *MYB* gene. The *HMIP* block 1, 2, and 3 are shown above indicated by the horizontal brackets. The figure also includes conserved GATA-1 motifs (●) and DNase I hypersensitive sites (↓) as identified in hemin-induced K562 cells.

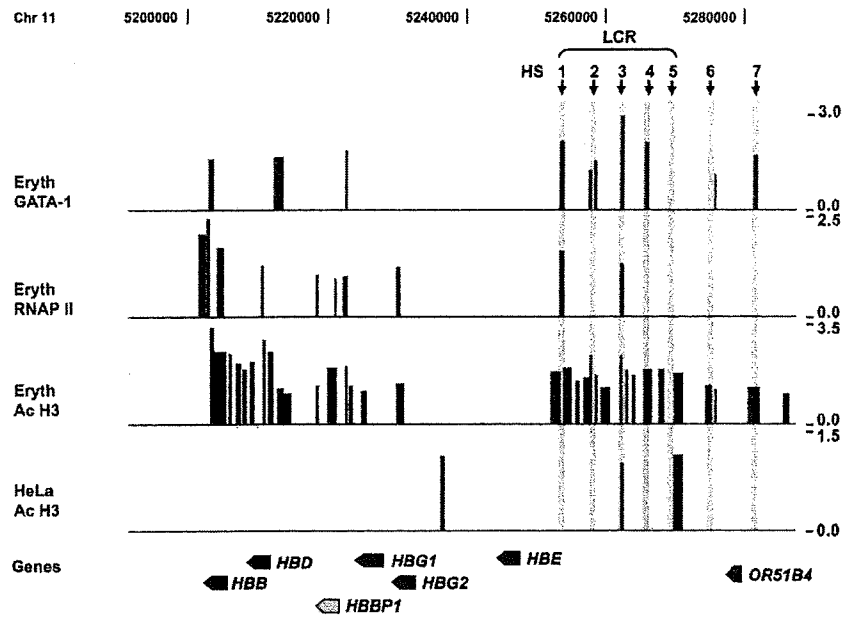

Figure 4. ChIP-chip data for the β globin locus in erythroid precursor and HeLa cells. Results from ChIP-chip experiments for GATA-1, RNAP II, and AcH3 in erythroid precursors and AcH3 in HeLa cells analyzed on the custom designed array. The figure covers a 120-kb region (position chr11: 5 180 000-5 302 000) that includes the entire β globin locus. The globin genes are indicated below and include β globin *(HBB)*, δ globin *(HBD)*, γ globin *(HBG1* and *HBG2)* and ε globin *(HBE)*, and the βψ pseudogene *(HBBP1)*. The region also includes the olfactory gene *(OR51B4)*. Hypersensitive sites in the β-globin LCR (HS1-HS5) and the upstream HS6 and HS7 are marked with ↓.

By including the well-characterized α and β globin loci on our custom-designed array, we introduced positive controls for histone acetylation and GATA-1 binding in erythroid cells to evaluate the quality of our ChIP material and data analysis. In addition, the custom array allowed us to compare patterns of histone acetylation and transcription factor binding between the distal regulatory regions of the globin loci and the *HBS1L-MYB* intergenic interval that would facilitate the evaluation of the region upstream of *HBS1L* and *MYB* as a potential distal regulatory element. Interestingly, strong similarities in patterns of histone acetylation as well as GATA-1 and RNAP II interactions were observed between the *HMIP* block 2 and 3 regions and the α and β globin control regions.

In the β globin locus, 2 isolated domains of activity (AcH3 signals) were clearly discernable and these were concentrated around the β LCR and a region covering the β and δ globin genes *(HBB* and *HBD)* and the area around the βψ pseudogene *(HBBP1*; Figure 4). These 2 domains of activity were separated by an inactive domain comprising the ε globin *(HBE)* gene and the region up to the γ globin genes *(HBG1* and *2)*. This pattern was similar to previously published data of H3 acetylation in human erythroid precursors.[29] HeLa cells showed little signal for H3 acetylation in the β globin locus. Some signal was detected in the LCR at HS3 and HS5, and upstream of the γ-globin genes. Acetylation at HS5 in HeLa cells is consistent with this site being ubiquitously active.

Strong GATA-1 signal was detected in the β globin LCR at HS1, HS2, HS3, and HS4, and at the upstream hypersensitive sites 6 and 7. In addition, GATA-1 signals were observed upstream of the *HBD* and *HBBP1* as well as in *HBB*. A closer view revealed that the GATA-1 signal in *HBB* coincided with exon 3 (Figure 4), which has previously been shown to contain an enhancer element involved in the control of β globin expression.[30] RNAP II binding in the β globin locus coincided with GATA-1 signals at HS1 and HS3 and was also associated with *HBG1* and the adult globin genes. The strongest RNAP II signal was observed around *HBB*, consistent with high expression of β globin in erythroid precursors at the time of harvest.

The α globin locus showed strong H3 acetylation around the α globin genes and the upstream regulatory domain in erythroid precursors but not in HeLa cells (Figure 5). Consistent with previous observations,[26] we observed GATA-1 signals at HS48, HS40, HS33, and HS10 upstream of the α globin genes. GATA-1 signal was also found at the human orthologous region corresponding to the mouse HS12 (hoHS12) and at a site in-between the ζ globin *(HBZ)* and the *ψα2* pseudogene *(HBM)*. RNAP II signals were observed at the α globin promoters and the upstream elements HS-48 and HS-40, again consistent with previous observations.

Given the unusually high and concentrated levels of H3 acetylation and evidence of RNAPII binding in the intergenic region, we decided to investigate the intergenic region for evidence of transcription using a high-resolution tiling array (supplemental methods). Primary human erythroid precursor cells (phase II, days 3 and 5 liquid culture) from 2 individuals were analyzed. All samples gave essentially identical results. As expected, there is strong transcriptional activity at the exons of *MYB* and *HBS1L*, with relatively little in the introns. However, very strong and well-defined transcriptional activity was identified in the intergenic locus spanning *HMIP-2* and *-3*. In several areas, the signal intensity is even greater than from the *MYB* exons (Figure 6).

Discussion

Here, we provide a first characterization of the intergenic sequences upstream of the *HBS1L* and *MYB* genes, strongly supporting the hypothesis of a regulatory region being located in this interval. The conclusion is supported by parallel analysis of histone acetylation, GATA-1, and RNAP II interaction patterns across the erythroid-specific α and β globin loci. Chromatin immunoprecipitation showed significant histone acetylation in the intergenic region in a restricted interval that encompasses *HMIP-2* and *-3* linkage disequilibrium blocks as defined from genetic analysis. The H3 acetylation was particularly well defined and concentrated in *HMIP-2*. Several GATA-1 binding sites were also identified in the *HBS1L-MYB* intergenic interval; within *HMIP-2*, all the GATA-1 signals coincided with the 3 DNase I hypersensitive sites identified in induced K562 cells, providing strong support for the sites being active regulatory elements in erythroid cells. Interestingly some of the GATA-1 sites also coincided with weak RNAP II binding. Weak

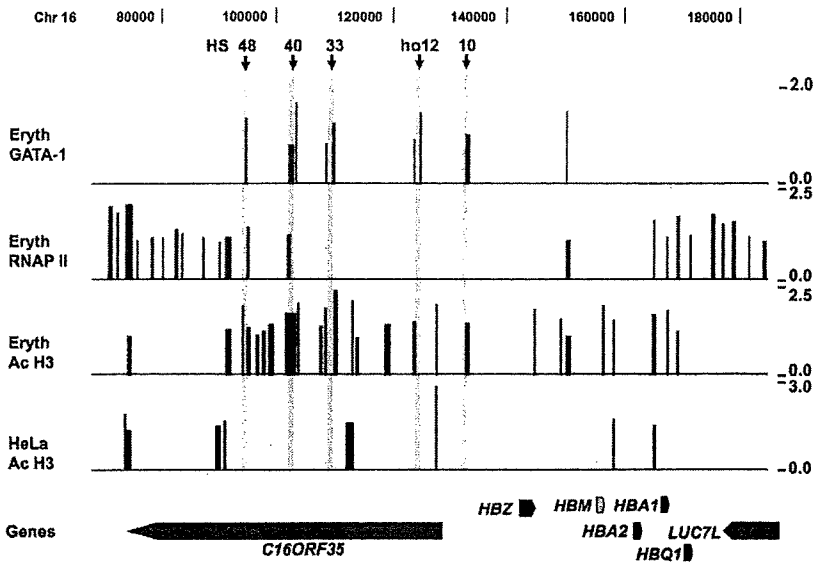

Figure 5. ChIP-chip data for the α globin locus in erythroid precursor and HeLa cells. Results from ChIP-chip experiments for GATA-1, RNAP II, and AcH3 in erythroid precursors and AcH3 in HeLa cells analyzed on the custom-designed array. The figure covers a 120-kb region (position chr16: 70 000-187 000) that includes the α-globin locus. The globin genes are indicated below and include ζ globin *(HBZ)*, α globins *(HBA1* and *HBA2)*, and θ globin *(HBQ1)*, and the ψα2 pseudogene *(HBM)*. Other genes include *C16ORF35* and *LUC7L*. Hypersensitive sites in the human α globin locus (HS48, HS40, HS33, and HS10) and the human orthologous mouse HS12 (ho12) are marked with ↓.

RNAP-II signals have previously been observed from ChIP-chip experiments at the site of enhancers and could be a marker of physical interactions with active promoters.[31] Such enhancer elements could affect distal transcriptional control via long-range physical interaction as supported by the observations of GATA-1 involvement in looping formation within the β globin locus. GATA-1, together with FOG-1, functions as an anchor in the formation of chromatin looping, and is required for physical interactions between the β LCR and β globin promoter.[32]

We show that the pattern of H3 acetylation in the *HBS1L-MYB* region differs between erythroid precursors and HeLa cells. HeLa cells that do not express hematopoietic transcription factors,

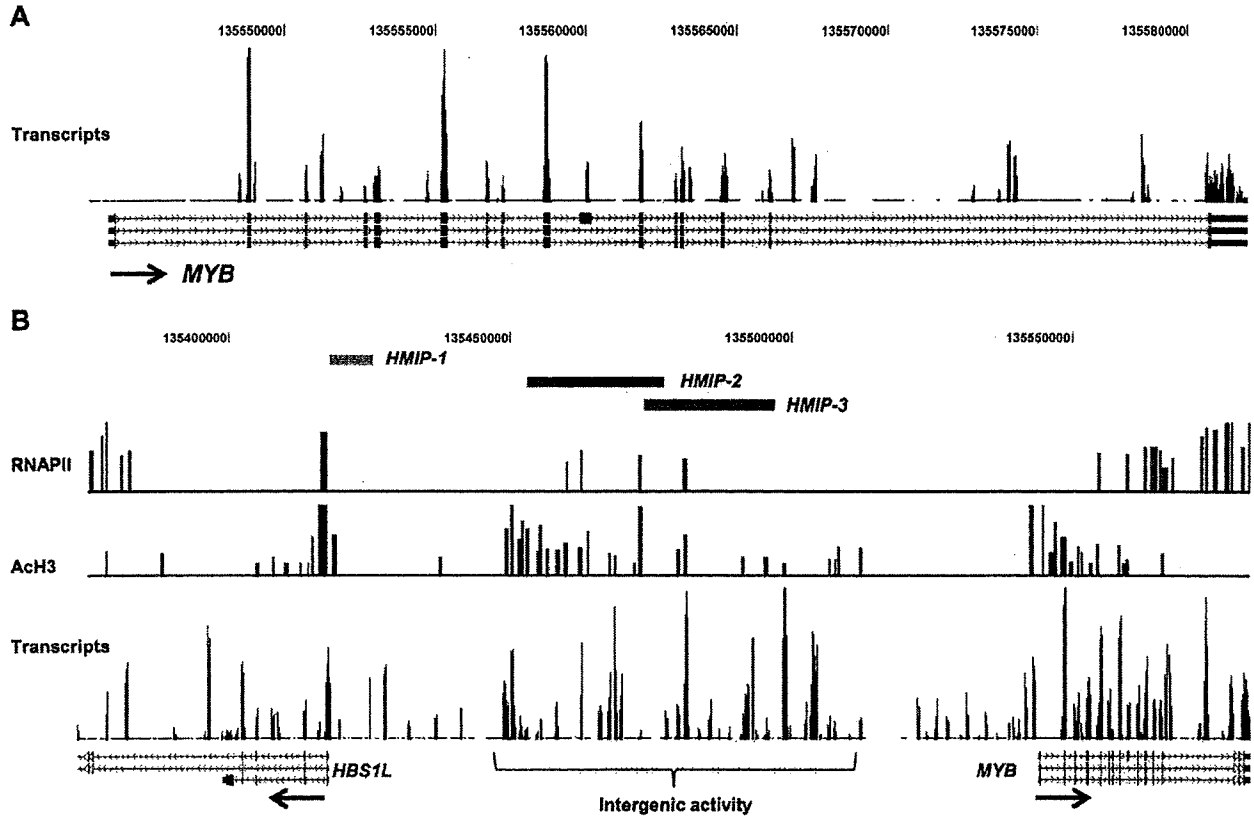

Figure 6. Transcript tiling array data from erythroid precursor cells. Results from 1 representative experiment are presented. (A) Transcript signal from the *MYB* genomic region shows very clear activity in exons and demonstrates that the array design and methodology are robust, given that *MYB* is highly expressed in the cells used. Occasional strong intronic signals were not coincident with spliced or unspliced ESTs and may therefore represent uncharacterized control elements or ncRNA. (B) Transcript data including *HBS1L*, *MYB*, and the intergenic region. The HbF-associated *HMIP* blocks 1 and 2 cover a region of high transcriptional activity. Again, there is no evidence of either spliced or unspliced ESTs. Given their magnitude in relation to the *MYB* signals and their complete consistency between different cultures tested, the intergenic signals are likely to represent important regulatory sequences.

including *MYB*, showed substantially less H3 acetylation in the intergenic region, suggesting a link between activity in the region and *MYB* expression. We identified a restricted peak of H3 acetylation in the intergenic region in HeLa cells that coincided with GATA-1 signal in erythroid precursors and HMHS3 in induced K562 cells. It is possible that this peak represents a basal level of chromatin acetylation and could conceivably be the crucial activation core for the locus in erythroid cells. Binding of specific transcription factors including GATA-1 to this site could lead to the activation of the regulatory region with consequent induction of expression of *MYB* and other genes in the domain.

Our study has also provided, for the first time, a large-scale analysis of GATA-1 occupancy in human erythroid cells. The abundant GATA-1 signals over the entire 70-Mb interval of chromosome 6q suggest that GATA-1 has an important regulatory role in erythroid cells. The powerful influence of GATA-1 on erythroid commitment and development was recently suggested in overexpression studies of GATA-1 that resulted in the transformation of HeLa cells to a more erythroid phenotype, including formation of the β globin LCR and expression of globin mRNA.[33] Our findings are supportive of GATA-1 having a role as a general transcription factor in erythroid cells in regulating the transcription of ubiquitous as well as erythroid-specific genes.

The identification of high levels of intergenic transcription provides further evidence that the *HBS1L-MYB* region contains a distal regulatory locus. Except for *HBS1L*-exon 1a, there is no evidence of ESTs, spliced or unspliced, or GeneScan gene predictions in the region (NCBI database; http://www.ncbi.nlm.nih.gov[34]), suggesting there are no undiscovered genes in the interval. Several studies on locus control regions have suggested that intergenic transcription may be involved in chromatin decondensation and looping, which is fundamental to gene activation. Alternatively, it may represent a "tracking" mechanism that enables a transcription complex to move along the locus until a transcriptionally competent promoter is encountered.[29,35,36] The patterns of histone acetylation, RNAP II binding, and GATA-1 interactions, in coincidence with the multiple DNase I hypersensitive sites and the intergenic transcripts in this defined interval, are highly similar to previously well-characterized erythroid control regions.

The regulatory potential of the region upstream of the *MYB* region and its influence on *MYB* expression has previously been emphasized. In murine models, *Myb* has been shown to be a key target for transcriptional activation by long-range upstream and downstream retroviral insertion.[37] Integration of proviruses in a region 25- to 90-kb upstream of *Myb* in mice is associated with tumorigenesis, suggesting a functional importance of these sequences.[38] Further, it has been observed that increased expression of the flanking genes occurred only in the presence of *Myb* overexpression. The observations suggest the possibility that regulation of *Myb* may affect a wider chromatin domain surrounding the gene. Alternatively, there may be common transcription factors or a common *cis*-regulatory element(s) that controls the expression of *Myb* and another gene(s) in its vicinity.[37] Further evidence supporting the regulatory potential of this region comes from a serendipitous insertion of a transgene in this intergenic region, 77-kb upstream of the mouse *Myb* gene, that resulted in reduced *Myb* expression and markedly decreased megakaryocyte/erythrocyte lineage-restricted progenitors of the homozygous mutant mice.[39]

Previously, we showed that *MYB* is a quantitative trait gene, with variable expression in healthy adults.[11] Our previous studies also showed that human erythroid precursor cells from individuals with higher HbF and higher F cell levels have lower *MYB* expression that was also associated with lower erythrocyte count but higher erythrocyte volume, and higher platelet count.[11] Further, mouse models in which *Myb* activity was reduced, due to either mutation or integration of a transgene near the *Myb* locus, displayed anemia and thrombocytosis.[39-44] It is clear that MYB, a transcription factor that is also involved in oncogenesis, has multiple essential roles throughout the different stages of erythropoiesis.

What is not clear, however, are the regulatory sequences controlling *MYB* expression. Recent studies show that *MYB* is a major target of the microRNA 150 (miR-150), and that one pathway of *MYB* regulation is through the 2 conserved miR-150 binding sites in the 3′ UTR of *MYB* mRNA.[45] miR-150 repression of *MYB* in $CD34^+$ human bone marrow cells not only supported *MYB*'s key role in erythroid and megakaryocytic differentiation, but also suggested that modulations of its level are critical to its role.[45] We propose that the *HBS1L-MYB* region upstream of *MYB* contains distal regulatory elements that form a key part of the overall control of *MYB* expression. The intergenic variants may account for some of the *cis*-control of the intrinsic quantitative variation in *MYB* expression. Genetic variants in the *HBS1L-MYB* interval on chromosome 6q have been shown to be highly associated, not only with HbF levels, but also with the control of other hematologic parameters. Taken together, our data have provided a functional basis for this association and strongly support the hypothesis of a regulatory locus upstream of the *HBS1L* and *MYB* genes, located within *HMIP-2* and *-3* blocks as identified in genetic association studies.

Delineation of the key variants in this *HBS1L-MYB* control region may lead to an improved understanding of *MYB* control and dysregulation[46] that underlies many of the leukemias and cancers, and may also provide targets for therapeutic activation of HbF[47] in the treatment of sickle cell disease and β thalassemia.

Acknowledgments

We thank Claire Steward for help in preparation of the manuscript; Drs Marco de Gobbi, Jim Hughes and David Garrick for their help with ChIP-chip experiments, and Dr Mike Antoniou, Dr Stephan Menzel, Professors Doug Higgs and Bill Wood for helpful discussions.

This work was supported by a grant from the Medical Research Council, United Kingdom (MRC G0000111 and ID51640) to S.L.T. and an MRC training studentship to K.W. The research at the Center for Genomic Medicine, Kyoto University, is partly supported by the Ministry of Education, Culture, Sports, Science and Technology of Japan. We also thank the London University Central Research Fund (CRF) and British Society for Hematology for support (S.B.).

Authorship

Contribution: K.W. performed research, analyzed data, and wrote the paper; J.J., H.R., K.J., F.M., and M.Y. performed research; M.L. contributed to data analysis and writing of the paper; S.L.T. codirected research and wrote the paper; and S.B. codirected research, analyzed data, and wrote the paper.

Conflict-of-interest disclosure: The authors declare no competing financial interests.

Correspondence: Swee Lay Thein, King's College London School of Medicine, James Black Centre, 125 Coldharbour Lane, London SE5 9NU, United Kingdom; e-mail: sl.thein@kcl.ac.uk.

References

1. Platt OS, Brambilla DJ, Rosse WF, et al. Mortality in sickle cell disease: life expectancy and risk factors for early death. *N Engl J Med.* 1994;330(23): 1639-1644.
2. Ho PJ, Hall GW, Luo LY, Weatherall DJ, Thein SL. Beta thalassemia intermedia: is it possible to consistently predict phenotype from genotype? *Br J Haematol.* 1998;100(1):70-78.
3. Weatherall DJ, Clegg JB. The Thalassaemia Syndromes. 4th Ed. Oxford, United Kingdom: Blackwell Science; 2001.
4. Garner C, Tatu T, Reittie JE, et al. Genetic influences on F cells and other hematologic variables: a twin heritability study. *Blood.* 2000;95(1):342-346.
5. Menzel S, Garner C, Gut I, et al. A QTL influencing F cell production maps to a gene encoding a zinc-finger protein on chromosome 2p15. *Nat Genet.* 2007;39(10):1197-1199.
6. Lettre G, Sankaran VG, Bezerra MA, et al. DNA polymorphisms at the BCL11A, *HBS1L-MYB*, and beta-globin loci associate with fetal hemoglobin levels and pain crises in sickle cell disease. *Proc Natl Acad Sci U S A.* 2008;105(33):11869-11874.
7. Sedgewick AE, Timofeev N, Sebastiani P, et al. BCL11A is a major HbF quantitative trait locus in three different populations with beta-hemoglobinopathies. *Blood Cells Mol Dis.* 2008;41(3):255-258.
8. Thein SL, Menzel S, Peng X, et al. Intergenic variants of HBS1L-MYB are responsible for a major quantitative trait locus on chromosome 6q23 influencing fetal hemoglobin levels in adults. *Proc Natl Acad Sci U S A.* 2007;104(23):11346-11351.
9. Uda M, Galanello R, Sanna S, et al. Genome-wide association study shows BCL11A associated with persistent fetal hemoglobin and amelioration of the phenotype of beta-thalassemia. *Proc Natl Acad Sci U S A.* 2008;105(3):1620-1625.
10. So CC, Song YQ, Tsang ST, et al. The HBS1L-MYB intergenic region on chromosome 6q23 is a quantitative trait locus controlling fetal haemoglobin level in carriers of beta-thalassaemia. *J Med Genet.* 2008;45(11):745-751.
11. Jiang J, Best S, Menzel S, et al. cMYB is involved in the regulation of fetal hemoglobin production in adults. *Blood.* 2006;108(3):1077-1083.
12. Menzel S, Jiang J, Silver N, et al. The HBS1L-MYB intergenic region on chromosome 6q23.3 influences erythrocyte, platelet, and monocyte counts in humans. *Blood.* 2007;110(10):3624-3626.
13. Wallrapp C, Verrier S-B, Zhouravleva G, et al. The product of the mammalian orthologue of the Saccharomyces cerevisiae HBS1 gene is phylogenetically related to eukaryotic release factor 3 (eRF3) but does not carry eRF3-like activity. *FEBS Lett.* 1998;440(3):387-392.
14. Oh IH, Reddy EP. The myb gene family in cell growth, differentiation and apoptosis. *Oncogene.* 1999;18(19):3017-3033.
15. Cantor AB, Orkin SH. Transcriptional regulation of erythropoiesis: an affair involving multiple partners. *Oncogene.* 2002;21(21):3368-3376.
16. Vegiopoulos A, Garcia P, Emambokus N, Frampton J. Coordination of erythropoiesis by the transcription factor c-Myb. *Blood.* 2006;107(12): 4703-4710.
17. Fibach E, Manor D, Oppenheim A, Rachmilewitz EA. Proliferation and maturation of human erythroid progenitors in liquid culture. *Blood.* 1989; 73(1):100-103.
18. McArthur M, Gerum S, Stamatoyannopoulos G. Quantification of DNaseI-sensitivity by real-time PCR: quantitative analysis of DNaseI-hypersensitivity of the mouse beta-globin LCR. *J Mol Biol.* 2001;313(1):27-34.
19. Dorschner MO, Hawrylycz M, Humbert R, et al. High-throughput localization of functional elements by quantitative chromatin profiling. *Nat Methods.* 2004;1(3):219-225.
20. National Center for Biotechnology Information. Gene Expression Omnibus (GEO). http://www.ncbi.nlm.nih.gov/geo. Accessed June 2, 2009.
21. O'Geen H, Nicolet CM, Blahnik K, Green R, Farnham PJ. Comparison of sample preparation methods for ChIP-chip assays. *Biotechniques.* 2006;41(5):577-580.
22. Kapranov P, Drenkow J, Cheng J, et al. Examples of the complex architecture of the human transcriptome revealed by RACE and high-density tiling arrays. *Genome Res.* 2005;15(17):987-997.
23. National Center for Biotechnology Information. Build 36. http://www.ncbi.nlm.nih.gov/mapview/map_search.cgi?taxid=10090. Accessed March 14, 2007.
24. Eisbruch A, Blick M, Evinger-Hodges MJ, et al. Effect of differentiation-inducing agents on oncogene expression in a chronic myelogenous leukemia cell line. *Cancer.* 1988;62(6):1171-1178.
25. Villeval JL, Pelicci PG, Tabilio A, et al. Erythroid properties of K562 cells: effect of hemin, butyrate and TPA induction. *Exp Cell Res.* 1983;146(2): 428-435.
26. De Gobbi M, Anguita E, Hughes J, et al. Tissue-specific histone modification and transcription factor binding in {alpha} globin gene expression. *Blood.* 2007;110(13):4503-4510.
27. University of California Santa Cruz. UCSC Genome Browser. http://genome.ucsc.edu. Accessed May 15, 2008.
28. Lian Z, Karpikov A, Lian J, et al. A genomic analysis of RNA polymerase II modification and chromatin architecture related to 3′ end RNA polyadenylation. *Genome Res.* 2008;18(8):1224-1237.
29. Miles J, Mitchell JA, Chakalova L, et al. Intergenic transcription, cell-cycle and the developmentally regulated epigenetic profile of the human beta-globin locus. *PLoS ONE.* (htttp://www.ncbi.nlm.nih.gov/entrez/query.fcgi?) 2007;2(7):e630.
30. Behringer RR, Hammer RE, Brinster RL, Palmiter RD, Townes TM. Two 3′ sequences direct adult erythroid-specific expression of human β-globin genes in transgenic mice. *Proc Natl Acad Sci U S A.* 1987;84(20):7056-7060.
31. Heintzman ND, Stuart RK, Hon G, et al. Distinct and predictive chromatin signatures of transcriptional promoters and enhancers in the human genome. *Nat Genet.* 2007;39(3):311-318.
32. Vakoc CR, Letting DL, Gheldof N, et al. Proximity among distant regulatory elements at the beta-globin locus requires GATA-1 and FOG-1. *Mol Cell.* 2005;17(3):453-462.
33. Layon ME, Ackley CJ, West RJ, Lowrey CH. Expression of GATA-1 in a non-hematopoietic cell line induces beta-globin locus control region chromatin structure remodeling and an erythroid pattern of gene expression. *J Mol Biol.* 2007;366(3): 737-744.
34. National Center for Biotechnology Information. http://www.ncbi.nlm.nih.gov. Accessed February 20, 2009.
35. Ashe HL, Monks J, Wijgerde M, Fraser P, Proudfoot NJ. Intergenic transcription and transinduction of the human β-globin locus. *Genes Dev.* 1997;11(19):2494-2509.
36. Gribnau J, Diderich K, Pruzina S, Calzolari R, Fraser P. Intergenic transcription and developmental remodeling of chromatin subdomains in the human beta-globin locus. *Mol Cell.* 2000;5(2): 377-386.
37. Hanlon L, Barr NI, Blyth K, et al. Long-range effects of retroviral insertion on c-myb: overexpression may be obscured by silencing during tumor growth in vitro. *J Virol.* 2003;77(2):1059-1068.
38. Haviernik P, Festin SM, Opavsky R, et al. Linkage on chromosome 10 of several murine retroviral integration loci associated with leukaemia. *J Gen Virol.* 2002;83(4):819-827.
39. Mukai HY, Motohashi H, Ohneda O, Suzuki N, Nagano M, Yamamoto M. Transgene insertion in proximity to thec-myb gene disrupts erythroid-megakaryocytic lineage bifurcation. *Mol Cell Biol.* 2006;26(21):7953-7965.
40. Mucenski ML, McLain K, Kier AB, et al. A functional c-myb gene is required for normal murine fetal hepatic hematopoiesis. *Cell.* 1991;65(4): 677-689.
41. Emambokus N, Vegiopoulos A, Harman B, Jenkinson E, Anderson G, Frampton J. Progression through key stages of haemopoiesis is dependent on distinct threshold levels of c-Myb. *EMBO J.* 2003;22(17):4478-4488.
42. Carpinelli MR, Hilton DJ, Metcalf D, et al. Suppressor screen in Mpl−/− mice: c-Myb mutation causes supraphysiological production of platelets in the absence of thrombopoietin signaling. *Proc Natl Acad Sci U S A.* 2004;101(17):6553-6558.
43. Sandberg ML, Sutton SE, Pletcher MT, et al. c-Myb and p300 regulate hematopoietic stem cell proliferation and differentiation. *Dev Cell.* 2005; 8(2):153-166.
44. Kasper LH, Boussouar F, Ney PA, et al. A transcription-factor-binding surface of coactivator p300 is required for haematopoiesis. *Nature.* 2002;419(6908):738-743.
45. Lu J, Guo S, Ebert BL, et al. MicroRNA-mediated control of cell fate in megakaryocyte-erythrocyte progenitors. *Dev Cell.* 2008;14(6):843-853.
46. García P, Frampton J. Hematopoietic lineage commitment: miRNAs add specificity to a widely expressed transcription factor. *Dev Cell.* 2008; 14(6):815-816.
47. Perrine SP. Hemoglobin F: new targets, new path. *Blood.* 2006;108(3):783-784.

Histological Course of Nonalcoholic Fatty Liver Disease in Japanese Patients

Tight glycemic control, rather than weight reduction, ameliorates liver fibrosis

ERIKA HAMAGUCHI, MD, PHD[1]
TOSHINARI TAKAMURA, MD, PHD[1]
MASARU SAKURAI, MD, PHD[2]
EISHIRO MIZUKOSHI, MD, PHD[3]
YOH ZEN, MD, PHD[4]
YUMIE TAKESHITA, MD, PHD[1]
SEIICHIRO KURITA, MD, PHD[1]
KUNIAKI ARAI, MD, PHD[3]
TATSUYA YAMASHITA, MD, PHD[3]
MOTOKO SASAKI, MD, PHD[5]
YASUNI NAKANUMA, MD, PHD[5]
SHUICHI KANEKO, MD, PHD[3]

OBJECTIVE — The goal of this study was to examine whether metabolic abnormalities are responsible for the histological changes observed in Japanese patients with nonalcoholic fatty liver disease (NAFLD) who have undergone serial liver biopsies.

RESEARCH DESIGN AND METHODS — In total, 39 patients had undergone consecutive liver biopsies. Changes in their clinical data were analyzed, and biopsy specimens were scored histologically for stage.

RESULTS — The median follow-up time was 2.4 years (range 1.0–8.5). Liver fibrosis had improved in 12 patients (30.7%), progressed in 11 patients (28.2%), and remained unchanged in 16 patients (41%). In a Cox proportional hazard model, decrease in A1C and use of insulin were associated with improvement of liver fibrosis independent of age, sex, and BMI. However, ΔA1C was more strongly associated with the improvement of liver fibrosis than use of insulin after adjustment for each other (χ^2; 7.97 vs. 4.58, respectively).

CONCLUSIONS — Tight glycemic control may prevent histological progression in Japanese patients with NAFLD.

Diabetes Care 33:284–286, 2010

Accumulating trans-sectional evidence suggests that the presence of multiple metabolic disorders, including obesity, diabetes, dyslipidemia, hypertension, and ultimately metabolic syndrome, are associated with nonalcoholic fatty liver disease (NAFLD) (1). However, it remains unclear which metabolic abnormalities are responsible for the pathological progression of NAFLD, especially in Japanese patients, who generally are not severely obese compared with Western patients.

We retrospectively compared clinical features with the histological changes in the livers of Japanese patients with NAFLD who had undergone serial liver biopsies.

RESEARCH DESIGN AND METHODS

— We recruited 195 patients with clinically suspected NAFLD who had undergone liver biopsies at Kanazawa University Hospital from 1997 through 2008. For details about the study subjects and the exclusion criteria, see supplementary Fig. 1 in the online appendix, available at http://care.diabetesjournals.org/cgi/content/full/dc09-0148/DC1. Of 178 patients diagnosed histologically as having NAFLD, 39 had undergone serial liver biopsies.

Data collection

Clinical information, including age, sex, body measurements, and prevalence of metabolic abnormalities, was obtained for each patient. Venous blood samples drawn for laboratory testing before the liver biopsies were obtained. All subjects had been administered a 75-g oral glucose tolerance test at baseline and at follow-up.

Liver biopsies

Biopsies were obtained after a thorough clinical evaluation and receipt of signed informed consent from each patient. All biopsies were analyzed twice and at separate times randomly by a single pathologist who was blinded to the clinical information and the order in which the biopsies were obtained. The biopsied tissues were scored for steatosis, stage, and grade as described (2), according to the standard criteria for grading and staging of nonalcoholic steatohepatitis proposed by Brunt et al. (3).

For additional details on subjects, data collection methods, liver pathology, and statistical analyses, see supplementary Methods in the online appendix.

RESULTS

— The basal clinical and biochemical data from 39 patients with NAFLD are described in supplementary Table 1. Prevalence of type 2 diabetes, hypertension, and dyslipidemia were 77, 36, and 64%, respectively. The median follow-up period was 2.4 years (range 1.0–8.5). Medications for diabetes and medication changes during the follow-up period are described in supplementary Table 2. Seventeen patients treated with oral diabetic agents were switched to insulin therapy after the initial biopsy. No patients initiated pioglitazone during follow-up.

From the [1]Department of Disease Control and Homeostasis, Kanazawa University Graduate School of Medical Science, Ishikawa, Japan; the [2]Department of Epidemiology and Public Health, Kanazawa Medical University, Ishikawa, Japan; the [3]Department of Gastroenterology, Kanazawa University Hospital, Ishikawa, Japan; the [4]Division of Pathology, Kanazawa University Hospital, Ishikawa, Japan; and the [5]Department of Human Pathology, Kanazawa University Graduate School of Medical Science, Ishikawa, Japan.
Corresponding author: Toshinari Takamura, ttakamura@m-kanazawa.jp.
Received 8 February 2009 and accepted 20 October 2009. Published ahead of print at http://care.diabetesjournals.org on 30 October 2009. DOI: 10.2337/dc09-0148.

Table 1—*Baseline and follow-up clinical features and gradients of laboratory markers associated with changes in liver fibrosis in 39 patients with NAFLD*

	Baseline				Follow-up			
	Improved	Stable	Progressed	*P*	Improved	Stable	Progressed	*P*
n	12	16	11		12	16	11	—
Simple fatty liver/nonalcoholic steatohepatitis (*n*)	3:9	9:7	10:1		10:2	9:7	6:5	
Age (years)	51.5 (29–66)	48.5 (20–79)	51.5 (29–66)	0.97				
Sex (M:F)	5:7	12:4	5:7	0.17				
BMI (kg/m^2)	27.5 (23.2–34.1)	27.7 (22.5–44.4)	30.9 (23.4–37.7)	0.74	26.9 (22.8–31.2)	29.1 (24.3–44.8)	30.7 (24.1–36.3)	0.13
Aspartate transaminase (IU/l)	70 (11–106)	29 (14–86)	32 (13–83)	0.05	23 (11–28)	26 (15–71)	24 (14–164)	0.20
Alanine transaminase (IU/l)	71 (10–209)	48 (23–81)	40 (11–162)	0.13	21 (11–53)	36 (21–66)	31 (12–202)	0.10
Fasting plasma glucose (mg/dl)	133 (96–207)	143 (87–414)	111 (76–167)	0.20	103 (93–220)	121 (83–198)	116 (88–199)	0.51
A1C (%)	8.2 (4.7–11.6)	8.0 (4.9–13.6)	6.2 (5.1–9.5)	0.27	6.0 (5.0–9.0)	6.2 (5.0–10.0)	7.0 (6.0–11.0)	0.10
HOMA-IR	3.9 (0.7–5.5)	3.4 (1.9–7.7)	3.9 (1.6–11.1)	0.91	3.1 (1.5–8.5)	3.4 (1.9–7.7)	3.9 (1.6–11.1)	0.76
QUICKI	0.32 (0.29–0.40)	0.31 (0.27–0.34)	0.31 (0.29–0.35)	0.32	0.33 (0.28–0.37)	0.32 (0.30–0.35)	0.31 (0.29–0.34)	0.82
Muscle insulin resistance	2.1 (1.5–4.0)	1.7 (0.3–3.3)	3.0 (2.1–4.4)	0.20	2.0 (1.3–5.9)	2.4 (1.6–4.5)	1.9 (1.3–4.5)	0.80
Hepatic insulin resistance ($\times 10^5$)	5.3 (2.3–10.2)	5.0 (2.3–10.0)	3.7 (1.4–10.6)	0.66	3.9 (1.4–9.8)	4.3 (1.9–15.9)	4.5 (2.3–8.8)	0.75
Total cholesterol (mg/dl)	191 (128–276)	187 (129–252)	206 (163–244)	0.57	192 (114–224)	195 (136–273)	194 (162–234)	0.74
Triglycerides (mg/dl)	111 (28–224)	114 (36–204)	96 (36–521)	0.87	104 (22–241)	115 (57–241)	131 (36–173)	0.68
HDL cholesterol (mg/dl)	47 (35–82)	51 (31–73)	48 (20–74)	0.68	53 (40–71)	52 (39–64)	52 (36–79)	0.92
Platelets ($\times 10^4/\mu$l)	21.1 (9.4–30.8)	23.0 (7.0–38.2)	24.3 (20.2–41.2)	0.29	23.3 (14.5–27.6)	21.5 (6.3–31.8)	24.0 (15.2–32.6)	0.60
Ferritin (μg/dl)	185 (13–452)	397 (190–604)	46 (10–347)	0.14	74 (16–211)	162 (110–614)	62 (10–171)	0.05
hs-CRP	0.40 (0.08–7.53)	0.14 (0.02–0.61)	0.06 (0.00–0.30)	0.23	0.09 (0.04–0.23)	0.10 (0.00–0.24)	0.09 (0.00–0.89)	0.89
Type IV collagen 7S (ng/dl)	5.1 (2.7–10.0)	4.1 (3.1–7.2)	3.7 (3.3–4.5)	0.27	3.5 (2.3–3.9)	8.3 (3.2–14.0)	4.0 (3.2–5.0)	0.21
HA (ng/dl)	20.6 (0.0–144.7)	25.5 (11.5–299)	30.4 (0.0–61.7)	0.66	32.8 (0.0–117.2)	24.5 (0.0–570)	24.3 (0.0–140.3)	0.63
P-III-P (U/ml)	0.6 (0.5–1.2)	0.6 (0.4–45.0)	0.5 (0.4–0.6)	0.07	0.6 (0.3–0.8)	0.5 (0.5–233.0)	0.6 (0.4–1.0)	0.96
Diabetes (%)	82	69	64	0.59	82	75	64	0.56
Dyslipidemia (%)	73	63	73	0.95	73	63	73	0.86
Hypertension (%)	64	18	36	0.03	64	18	36	0.10
Metabolic syndrome (%)	73	38	27	0.18	67	50	45	0.43
ΔA1C					−1.9 (−6.0 to 0.4)	−1.2 (−6.1 to 4.4)	0.3 (−1.8 to 7.1)	0.02
ΔBody weight					−4.7 (−10.6 to 10.2)	2.2 (−9.4 to 13.4)	−0.9 (−12.7 to 9.6)	0.04
ΔHOMA-IR					−1.3 (−4.4 to 1.2)	−0.3 (−4.3 to 3.3)	−0.7 (−6.1 to 1.8)	0.81

Data are medians (range) or %. A Kruskal-Wallis test and a χ^2 test were used to compare the continuous and categorical variables among three groups. HA, hyaluronic acid; hs-CRP, high-sensitivity C-reactive protein; P-III-P, procollagen III peptide.

Liver fibrosis improved in 12 patients (30.7%), progressed in 11 patients (28.2%), and remained unchanged in 16 patients (41%). As shown in Table 1, fasting plasma glucose, A1C, insulin resistance indicators, and prevalence of metabolic disorders were not significantly different among the three liver fibrosis groups. In the Cox proportional hazard model (supplementary Table 3), although some of the confidence intervals were very wide because of the small sample size, improvement of liver fibrosis was significantly associated with changes in A1C between the initial and final liver biopsies (ΔA1C) ($P = 0.005$) and use of insulin for the treatment of diabetes ($P = 0.019$). Both ΔA1C and use of insulin were independently associated with the improvement of liver fibrosis after adjusted for each other. However, ΔA1C was more strongly associated with the improvement of liver fibrosis than use of insulin (χ^2; 7.97 vs. 4.58, respectively; supplementary Table 3).

CONCLUSIONS— In the present study, we showed that a change in glycemic control (ΔA1C), but not changes in insulin resistance indicators, was an independent predictor of the progression of liver fibrosis in Japanese patients with NAFLD. This is the first report identifying a change in A1C as a predictor of the histological course in the liver of patients with NAFLD. Two of five previous longitudinal studies have identified obesity, higher BMI, and homeostasis model assessment of insulin resistance (HOMA-IR) as predictors of liver fibrosis progression in Western populations (4,5). The difference between those results and the results of the present study may be due in part to differences in the assessed severity of obesity and insulin resistance between the populations. We previously demonstrated that diabetes is an independent risk factor for the progression of liver fibrosis in hepatitis C (6) and that diabetes accelerates the pathology of nonalcoholic steatohepatitis in the type 2 diabetic rat model OLETF (7).

Liver fibrosis is closely associated with two regulators of fibrosis: transforming growth factor (TGF)-β (8,9) and plasminogen activator inhibitor type 1 (PAI-1) (8,10). High glucose levels induce the expression of TGF-β (11) and PAI-1 (12). We previously reported that the expression of TGF family member genes, PAI-1, and genes involved in fibrogenesis are upregulated in the livers of patients with type 2 diabetes (13,14), suggesting that a diabetic state increases the risk for liver fibrosis.

In the present study, only ΔA1C was associated with the progression of liver fibrosis, but not liver inflammation (data not shown). We speculate that the reduction of A1C inhibits the expression of master genes such as *TGF-β* and *PAI-1* that are involved in the regulation of fibrogenesis, rather than genes involved in liver inflammation, and thereby improves liver fibrosis in NAFLD.

The major limitation of this study was small population size. We could not evaluate the changes of liver histology according to the difference in detail characteristics such as treatment of diabetes. Lower statistical power of this study should be consider when we evaluate the results.

In conclusion, our study suggested that ΔA1C could predict liver fibrosis progression in Japanese patients with NAFLD, and tight glycemic control may ameliorate liver fibrosis. Future large-scale prospective studies are needed to confirm our results.

Acknowledgments— This study was supported in part by a grant-in-aid from the Ministry of Education, Culture, Sports, Science and Technology, Japan.

No potential conflicts of interest relevant to this article were reported.

We thank Dr. Akiko Shimizu, Dr. Tsuguhito Ota, and Dr. Hirofumi Misu for recruiting the patients.

References

1. Duvnjak M, Lerotic I, Barsic N, Tomasic V, Virovic Jukic L, Velagic V. Pathogenesis and management issues for non-alcoholic fatty liver disease. World J Gastroenterol 2007;13:4539–4550
2. Sakurai M, Takamura T, Ota T, Ando H, Akahori H, Kaji K, Sasaki M, Nakanuma Y, Miura K, Kaneko S. Liver steatosis, but not fibrosis, is associated with insulin resistance in nonalcoholic fatty liver disease. J Gastroenterol 2007;42:312–317
3. Brunt EM, Janney CG, Di Bisceglie AM, Neuschwander-Tetri BA, Bacon BR. Nonalcoholic steatohepatitis: a proposal for grading and staging the histological lesions. Am J Gastroenterol 1999;94:2467–2474
4. Ekstedt M, Franzen LE, Mathiesen UL, Thorelius L, Holmqvist M, Bodemar G, Kechagias S. Long-term follow-up of patients with NAFLD and elevated liver enzymes. Hepatology 2006;44:865–873
5. Fassio E, Alvarez E, Dominguez N, Landeira G, Longo C. Natural history of nonalcoholic steatohepatitis: a longitudinal study of repeat liver biopsies. Hepatology 2004;40:820–826
6. Kita Y, Mizukoshi E, Takamura T, Sakurai M, Takata Y, Arai K, Yamashita T, Nakamoto Y, Kaneko S. Impact of diabetes mellitus on prognosis of patients infected with hepatitis C virus. Metabolism 2007;56:1682–1688
7. Ota T, Takamura T, Kurita S, Matsuzawa N, Kita Y, Uno M, Akahori H, Misu H, Sakurai M, Zen Y, Nakanuma Y, Kaneko S. Insulin resistance accelerates a dietary rat model of nonalcoholic steatohepatitis. Gastroenterology 2007;132:282–293
8. Matsuzawa N, Takamura T, Kurita S, Misu H, Ota T, Ando H, Yokoyama M, Honda M, Zen Y, Nakanuma Y, Miyamoto K, Kaneko S. Lipid-induced oxidative stress causes steatohepatitis in mice fed an atherogenic diet. Hepatology 2007;46:1392–1403
9. Uno M, Kurita S, Misu H, Ando H, Ota T, Matsuzawa-Nagata N, Kita Y, Nabemoto S, Akahori H, Zen Y, Nakanuma Y, Kaneko S, Takamura T. Tranilast, an antifibrogenic agent, ameliorates a dietary rat model of nonalcoholic steatohepatitis. Hepatology 2008;48:109–118
10. Bergheim I, Guo L, Davis MA, Lambert JC, Beier JI, Duveau I, Luyendyk JP, Roth RA, Arteel GE. Metformin prevents alcohol-induced liver injury in the mouse: critical role of plasminogen activator inhibitor-1. Gastroenterology 2006;130:2099–2112
11. Sugimoto R, Enjoji M, Kohjima M, Tsuruta S, Fukushima M, Iwao M, Sonta T, Kotoh K, Inoguchi T, Nakamuta M. High glucose stimulates hepatic stellate cells to proliferate and to produce collagen through free radical production and activation of mitogen-activated protein kinase. Liver Int 2005;25:1018–1026
12. Suzuki M, Akimoto K, Hattori Y. Glucose upregulates plasminogen activator inhibitor-1 gene expression in vascular smooth muscle cells. Life Sci 2002;72:59–66
13. Takamura T, Sakurai M, Ota T, Ando H, Honda M, Kaneko S. Genes for systemic vascular complications are differentially expressed in the livers of type 2 diabetic patients. Diabetologia 2004;47:638–647
14. Takeshita Y, Takamura T, Hamaguchi E, Shimizu A, Ota T, Sakurai M, Kaneko S. Tumor necrosis factor-alpha-induced production of plasminogen activator inhibitor 1 and its regulation by pioglitazone and cerivastatin in a nonmalignant human hepatocyte cell line. Metabolism 2006;55:1464–1472

Journal of Gerontology: BIOLOGICAL SCIENCES
Cite journal as: J Gerontol A Biol Sci Med Sci
2010 Vol. 65A, No. 1, 9–13
doi:10.1093/gerona/glp160

Advance Access published on October 27, 2009

Influence of Age on Clock Gene Expression in Peripheral Blood Cells of Healthy Women

Hitoshi Ando,[1] Kentarou Ushijima,[1] Masafumi Kumazaki,[2] Toshinari Takamura,[2] Noritsugu Yokota,[3] Tetsuo Saito,[3] Shin Irie,[4] Shuichi Kaneko,[2] and Akio Fujimura[1]

[1]Division of Clinical Pharmacology, Department of Pharmacology, School of Medicine, Jichi Medical University, Shimotsuke, Japan.
[2]Department of Disease Control and Homeostasis, Kanazawa University Graduate School of Medical Science, Japan.
[3]Moka Hospital, Japan.
[4]LTA Clinical Pharmacology Center, Medical Co.LTA, Fukuoka, Japan.

Recent studies have demonstrated a close relationship between circadian clock function and the development of obesity and various age-related diseases. In this study, we investigated whether messenger RNA (mRNA) levels of clock genes are associated with age, body mass index, blood pressures, fasting plasma glucose, or shift work. Peripheral blood cells were obtained from 70 healthy women, including 25 shift workers, at approximately 9:00 AM. Transcript levels of clock genes (*CLOCK*, *BMAL1*, *PER1*, and *PER3*) were determined by real-time quantitative polymerase chain reaction. Stepwise multiple regression analysis demonstrated that *BMAL1* mRNA levels were correlated only with age ($\beta = -.50$, $p < .001$). In contrast, *PER3* levels were correlated with fasting plasma glucose ($\beta = -.29$, $p < .05$) and shift work ($\beta = .31$, $p < .05$). These results suggest that increased age, glucose intolerance, and irregular hours independently affect the intracellular clock in humans.

Key Words: Aging—Biological clock—Circadian rhythm—Shift work.

BIOLOGICAL clocks represent an adaptation to daily 24-hour changes in the environment and enable organisms to maintain physiological homeostasis (1,2). The circadian clock resides in the hypothalamic suprachiasmatic nucleus (SCN), which is recognized as being the master clock. The same clock also exists in almost all peripheral tissues, including liver, heart, kidney (3,4), and blood cells (5,6). Although the SCN is not essential for driving peripheral oscillations, it appears to coordinate peripheral clocks (3).

The intracellular clock consists of autoregulatory transcriptional–translational feedback loops that have both positive and negative elements (1,2). The positive components are two basic helix–loop–helix transcription factors called CLOCK and brain and muscle Arnt-like protein 1 (BMAL1) (7,8). The heterodimer activates the transcription of several other clock genes, including Period (*PER*) and Cryptochrome (*CRY*) (9–11). The resultant PER and CRY proteins form a heterodimer, translocate to the nucleus, and inhibit the activity of CLOCK–BMAL1, thus forming a negative feedback loop. The intracellular clock is thought to directly and/or indirectly regulate the expression of numerous genes (1,2).

It has become evident that circadian clock function is important to the preservation of health. For example, a certain mutation in the *CLOCK* gene induces obesity and metabolic syndrome in mice (12), and genetic variations in the *BMAL1* and *CLOCK* genes are associated with susceptibility to obesity, hypertension, and type 2 diabetes in humans (13–15). Additionally, the *Per2* gene plays an important role in tumor suppression and DNA damage responses: *Per2* mutant mice are known to be cancer prone (16). Interestingly, several epidemiological studies have shown that shift work is associated with obesity, hypertriglyceridemia, glucose intolerance, hypertension, and breast cancer (17–20). Moreover, aging is known to be associated with a variety of alterations in circadian rhythms, which may contribute to various age-related diseases (21,22). It was previously shown that cellular senescence impairs circadian expression of clock genes in vitro (22). These findings raise the possibility that shift work and aging may cause various pathological conditions (e.g., obesity and cancer) through the impairment of biological clock function.

To date, the effects of aging and shift work on intracellular clocks remain to be determined. To address this issue, we measured the messenger RNA (mRNA) levels of *BMAL1*, *PER1*, and *PER3* in peripheral blood cells obtained from healthy women at approximately 9:00 AM, as indicators of overall clock function (6). We investigated the associations between the mRNA levels and age, shift work, body mass index (BMI), blood pressure, and fasting plasma glucose concentration.

Methods

Participants and Sampling

We recruited 70 healthy women (age range 20–79 years, median 53.5 years; BMI range 17.1–31.5 kg/m^2, median 22.2 kg/m^2) from the registered healthy volunteers at the clinical trial unit of LTA PS Clinic (Fukuoka, Japan) between December 2007 and April 2008 and the staff of Moka Hospital (Moka, Japan) between September and November 2008. Because mRNA levels of a subset of clock genes in

Table 1. Characteristics of Participants

	All Participants		Participants Who Kept Regular Hours		Shift Workers	
	n	*M* ± *SD* or %	*n*	*M* ± *SD* or %	*n*	*M* ± *SD* or %
Total	70		45		25	
Age (y)	70	52 ± 14	45	59 ± 11	25	40 ± 12**
Participants aged 65 y or older	15	21	14	31	1	4**
Postmenopausal women	40	57	36	80	4	16**
BMI (kg/m^2)	70	22.5 ± 3.0	45	22.4 ± 2.9	25	22.6 ± 3.2
Participants with BMI ≥25 kg/m^2	14	20	10	22	4	16
Systolic blood pressure (mmHg)	69	120 ± 12	44	121 ± 13	25	118 ± 10
Diastolic blood pressure (mmHg)	69	70 ± 9	44	71 ± 8	25	68 ± 9
Participants with blood pressure ≥140/90 mmHg	3	4	2	5	1	4
Fasting plasma glucose (mg/dL)	59	93 ± 9	44	94 ± 9	15	93 ± 10
Relative messenger RNA levels of clock genes						
CLOCK	70	1 ± 0.20	45	1.04 ± 0.21	25	0.93 ± 0.16*
BMAL1	70	1 ± 0.17	45	0.98 ± 0.16	25	1.04 ± 0.18
PER1	70	1 ± 0.51	45	0.92 ± 0.44	25	1.15 ± 0.58
PER3	70	1 ± 0.33	45	0.89 ± 0.23	25	1.19 ± 0.40**

Notes: BMI = body mass index.
*$p < .05$, **$p < .01$ versus participants who kept regular hours.

peripheral blood cells differ between men and women (unpublished data, 2009), only women were included. The following participants were excluded from the study: those who took any medications during the 2 weeks preceding the study; those who experienced jet lag in the preceding month; and those with a sleep disorder, inflammatory disease, malignancy, severe anemia (hemoglobin level <8.0 g/dL), diagnosed hypertension, or diabetes. This information was obtained by interviewing participants and by reviewing the medical records if available. Additional information about the lifestyles (sleep time and mealtimes) was also collected from all participants on the day of the study.

Physical measurements and venous blood sampling were performed between 8:30 and 9:30 AM following an overnight fast. Systolic and diastolic blood pressures were measured in a standardized manner. The samples for RNA isolation were collected into PAXgene Blood RNA tubes (Becton, Dickinson and Company Japan, Tokyo, Japan), and the tubes were incubated at room temperature for at least 4 hours and then stored at −80°C until RNA extraction. In all the 56 participants aged 40 years and older and 3 of 14 participants younger than 40 years, plasma glucose levels were measured using a commercial kit.

As shown in Table 1, 40 of the 70 participants were postmenopausal women. Fourteen participants were overweight or obese, three participants had mild hypertension (systolic and diastolic blood pressures: 143–145 and 86–87 mmHg, respectively), but none of the participants had diabetes (fasting plasma glucose ≥126 mg/dL). Twenty-five participants at Moka Hospital were shift workers and had worked through the night several times during the preceding month. The other 45 women had kept regular hours for at least 2 weeks prior to the beginning of the study, usually waking between 5:00 and 8:00 AM and retiring between 9:00 PM and 1:00 AM. Four participants did not eat breakfast, and three participants did not eat lunch. The other 38 typically consumed three meals per day.

This study was approved by the ethics committees of Jichi Medical University (Shimotsuke, Japan) and Medical Co. LTA (Fukuoka) and was conducted in accordance with the Declaration of Helsinki. Participants participated in the study only after providing their written informed consent.

RNA Extraction and Real-Time Quantitative Polymerase Chain Reaction

Total RNA isolation was achieved using a PAXgene Blood RNA kit (Qiagen Japan, Tokyo, Japan) according to the manufacturer's instruction. Complementary DNA (cDNA) was synthesized from 300 ng of total RNA using a High Capacity cDNA Reverse Transcription kit (Applied Biosystems Japan, Tokyo, Japan). Gene expression was analyzed by real-time quantitative polymerase chain reaction (PCR) using an Applied Biosystems' StepOnePlus Real-Time PCR system. All specific sets of primers and TaqMan probes (TaqMan Gene Expression Assays) were obtained from Applied Biosystems. To control for variation in the amount of cDNA available for PCR in the different samples, gene expression levels of the target sequences were normalized to the expression of an endogenous control, glyceraldehyde-3-phosphate dehydrogenase (*GAPDH*). The GenBank accession numbers, assay ID, and target exons were NM_004898.2, Hs00231857_m1, and 18-19 for *CLOCK*; NM_001178.4, Hs00154147_m1, and 9-10 for *BMAL1*; NM_002616.1, Hs00242988_m1, and 22-23 for *PER1*; NM_016831.1, Hs00213466_m1, and 15-16 for *PER3*; and NM_002046.3, Hs99999905_m1, and 3-3 for *GAPDH*, respectively. Data were analyzed using the comparative threshold cycle method.

Table 2. Correlation Coefficients Between Clock Gene Messenger RNA Levels and Variables

	CLOCK	*BMAL1*	*PER1*	*PER3*
All participants				
Age	0.15	−0.29*	−0.13	−0.41**
BMI	0.16	−0.05	−0.06	0.21
Systolic blood pressure	−0.03	−0.03	−0.07	−0.02
Diastolic blood pressure	0.19	0.18	−0.04	0.05
Fasting plasma glucose	−0.25	−0.10	0.01	−0.31*
Participants who kept regular hours				
Age	−0.06	−0.46**	0.24	−0.11
BMI	0.20	−0.05	0.05	0.26
Systolic blood pressure	−0.04	−0.12	−0.11	0.10
Diastolic blood pressure	0.19	0.12	−0.04	0.22
Fasting plasma glucose	−0.25	−0.07	0.17	−0.28
Shift workers				
Age	0.01	0.07	−0.27	−0.29
BMI	0.15	−0.06	−0.22	0.20
Systolic blood pressure	−0.12	0.19	0.06	−0.06
Diastolic blood pressure	0.07	0.35	0.04	0.06
Fasting plasma glucose	−0.42	−0.16	−0.49	−0.39

Notes: BMI = body mass index.
*$p < .05$, **$p < .01$.

Statistical Analysis

Associations between clock gene mRNA levels and age, BMI, and shift work were assessed using Pearson's correlation coefficient and stepwise multiple regression analysis. Differences between participants who kept regular hours and shift workers were assessed by chi-square and *t* tests. Statistical significance was defined as $p < .05$. All calculations were performed using SPSS version 11 for Windows (SPSS Japan, Tokyo, Japan).

Results

As shown in Table 1, the shift workers were significantly younger than the participants who kept regular hours. Consequently, there were fewer postmenopausal women in the shift worker group. However, BMI, blood pressures, and fasting plasma glucose concentration did not differ between the groups. The mRNA levels of *CLOCK* were slightly but significantly lower in the shift workers, whereas their *PER3* levels were higher than that in the other participants.

In the 45 women who were not shift workers, there was significant correlation between the mRNA levels of *BMAL1* and age (Table 2; $r = -.46$, $p < .01$). This negative correlation was also detected in all participants (Table 2 and Figure 1A; $r = -.29$, $p = .01$). *PER3*, but not the other clock genes examined, also correlated with age ($r = -.41$, $p < .001$). In addition, *PER3* negatively correlated with fasting plasma glucose ($r = -.31$, $p < .05$) in accord with our previous results (6). However, these correlations were not observed in the shift workers (Table 2). Contrary to expectation, none of the clock genes examined correlated with BMI and blood pressures in either the 45 participants who kept regular hours or the entire group of 70 participants (Table 2 and Figure 1B).

Because the shift workers were significantly younger than the others, we next performed stepwise multiple regression analysis with age, BMI, blood pressures, fasting plasma glucose, and shift work as independent variables and clock gene transcript levels as dependent variables. This analysis further demonstrated that *BMAL1* was correlated only with age ($R = .50$, $p < .001$; age, $\beta = -.50$, $p < .001$). Moreover, *PER3* mRNA levels were correlated with fasting

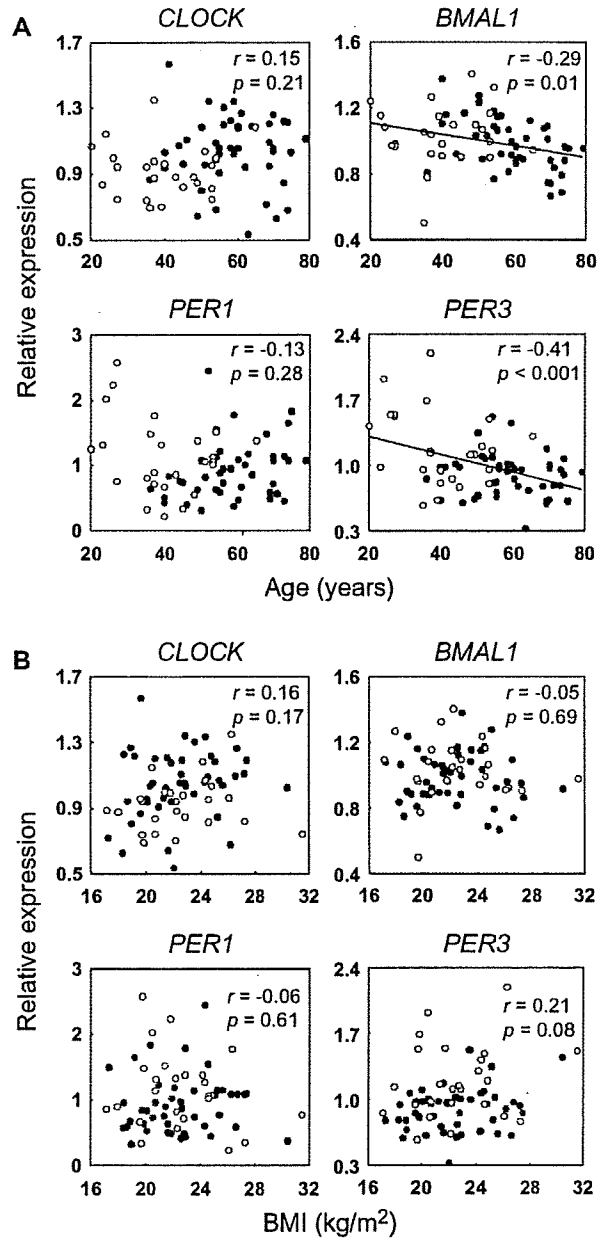

Figure 1. Relationship between messenger RNA levels of clock genes (*CLOCK*, *BMAL1*, *PER1*, and *PER3*) and age (A) or body mass index (BMI) (B) assessed using Pearson's correlation coefficient. Peripheral blood cells were obtained from 70 healthy women at approximately 9:00 AM. Twenty-five participants (white circles) were shift workers, and the other 45 women (black circles) kept regular hours for at least 2 weeks prior to the study. The transcript levels of clock genes were determined by real-time quantitative polymerase chain reaction. The mean value of all participants was set to 1 for each gene.

plasma glucose and shift work ($R = .44$, $p < .01$; fasting plasma glucose, $\beta = -.29$, $p < .05$; shift work, $\beta = .31$, $p < .05$). These results suggest that both age and shift work affect mRNA expression of a subset of clock genes.

Discussion

Here, we report for the first time a clear association between age and mRNA levels of *BMAL1*, which is a core element of the circadian clock, in humans. Although the rhythm of *BMAL1* expression in peripheral blood cells varies among individuals, *BMAL1* transcript levels often reach a trough level at the time specifically investigated in this study (5,6). Therefore, aging appears to affect *BMAL1* levels per se, rather than the phase of expression rhythms. Aging is known to influence the endocrine circadian system and the amplitudes of rhythms in particular. For example, secretion levels of various hormones, including cortisol, generally decrease in the elderly participants (23). It is speculated that the glucocorticoid signal is important for the oscillation of peripheral clocks as dexamethasone can reset them (24). In addition, age-associated decreases in nitric oxide production may also cause reversible impairment of the circadian clock (25). Furthermore, in this study, *BMAL1* levels in the postmenopausal participants were significantly lower than those in the menstruating women (data not shown). Thus, the age-related alterations in the endocrine circadian system may cause a reduction in the clock gene levels. Because at least part of the age-dependent disturbances of the circadian system can be reversed (26), the molecular machinery of intracellular clocks appears to be maintained even in advanced age. Further studies are needed to determine whether *BMAL1* levels correlate with circulating levels of some humoral factors including cortisol and nitric oxide or whether susceptibility to humoral cues decreases in the peripheral clocks of the elderly participants.

Previous studies from our laboratory have shown that the rhythmic expression of clock genes is blunted in both the liver and the visceral adipose tissues of obese diabetic mice (27) and in the peripheral leukocytes of patients with type 2 diabetes (6). In human leukocytes, the transcript levels of *BMAL1*, *PER1*, and *PER3* are inversely correlated with glycosylated hemoglobin levels (6). Given that several obesity-related humoral factors, including glucose (28), tumor necrosis factor α (29), and angiotensin II (30), can affect the circadian clock in vitro, it is possible that obesity alters the rhythmic expression of clock genes. Nevertheless, a significant association between BMI and clock gene expression was not detected in this study. The effect of mild simple obesity (without diabetes or hypertension) on circadian clock function in peripheral blood cells appears to be negligible.

Findings from recent studies suggest that circadian clock function plays a role in the development of obesity (12,14,15). However, the biological systems involved in body weight regulation are extremely complex, and many genes and chromosomal regions may contribute to defining the common obese phenotype (31). These genes are implicated in a wide variety of biological functions, including the regulation of food intake, energy expenditure, lipid and glucose metabolisms, and adipose tissue development (31). Therefore, it is not surprising that the association between BMI and clock gene expression was not detected in our small-scale study, even though such functions may be regulated by the biological clock.

Sleep–wake cycles have been shown to influence the rhythmic mRNA expression of clock genes in peripheral blood cells of healthy participants (32,33). Archer and colleagues (33) reported that *PER3* and *BMAL1* mRNA levels in peripheral blood cells of healthy participants were positively and negatively correlated with sleep time, respectively. The present study identified similar effects in people performing shift work. Several epidemiological studies suggest that shift work increases the risk of obesity, hypertriglyceridemia, glucose intolerance, hypertension, and breast cancer (17–20). As clock gene dysfunction is thought to cause these pathological conditions (12–16), impairment of the circadian clock may contribute to their subsequent development in shift workers. Further studies are needed to determine the degree of impairment in the clock oscillation system in shift workers.

In this study, we measured the transcript levels of clock genes at only one time point. In addition, daily rhythms of biological functions, such as core body temperature, and rhythmic expression of clock-controlled genes were not investigated. Therefore, it is not known exactly what the altered levels of clock genes indicate. However, the fact that altered mRNA levels of clock genes in peripheral blood cells obtained at an appropriate time point often indicate impaired expression rhythms of them has been revealed in patients with various diseases, including type 2 diabetes (6), circadian rhythm sleep disorder (34), and obstructive sleep apnea syndrome (35). In addition, the clock gene transcript levels in peripheral blood cells (36) and adipose tissues (37) obtained at a time point were reported to be correlated with the metabolic syndrome parameters. Therefore, the alternate measurement approach used in this study may be useful to assess the rhythm and/or function of circadian clock at least in peripheral tissues. Whether the altered clock gene levels in peripheral blood cells are associated with the development of various diseases should be determined in future studies.

In summary, the mRNA levels of a subset of clock genes in the peripheral blood cells of healthy women were found to correlate with age, fasting plasma glucose, and shift work. These results suggest that aging, like glucose intolerance and irregular hours, affects the rhythmic expression of clock genes in humans.

Funding

H.A. received Grants-in-Aid for Scientific Research (18790622 and 21790880) from the Ministry of Education, Culture, Sports, Science, and Technology of Japan and support from the Daiwa Securities Health Foundation and Eli Lilly Japan.

ACKNOWLEDGMENTS

We are grateful to all participants for their cooperation. We also thank T. Hayasaka, M. Ishibashi, M. Nagamizu, T. Shobu, and M. Kawagoe for their support.

CORRESPONDENCE

Address correspondence to Akio Fujimura, MD, PhD, Department of Pharmacology, School of Medicine, Jichi Medical University, 3311-1 Yakushiji, Shimotsuke, Tochigi 329-0498, Japan. Email: akiofuji@jichi.ac.jp

REFERENCES

1. Lowrey PL, Takahashi JS. Mammalian circadian biology: elucidating genome-wide levels of temporal organization. *Annu Rev Genomics Hum Genet.* 2004;5:407–441.
2. Reppert SM, Weaver DR. Coordination of circadian timing in mammals. *Nature.* 2002;418:935–941.
3. Yoo SH, Yamazaki S, Lowrey PL, et al. PERIOD2: LUCIFERASE real-time reporting of circadian dynamics reveals persistent circadian oscillations in mouse peripheral tissues. *Proc Natl Acad Sci U S A.* 2004;101:5339–5346.
4. Yamamoto T, Nakahata Y, Soma H, Akashi M, Mamine T, Takumi T. Transcriptional oscillation of canonical clock genes in mouse peripheral tissues. *BMC Mol Biol.* 2004;5:18.
5. Kusanagi H, Mishima K, Satoh K, Echizenya M, Katoh T, Shimizu T. Similar profiles in human period1 gene expression in peripheral mononuclear and polymorphonuclear cells. *Neurosci Lett.* 2004;365:124–127.
6. Ando H, Takamura T, Matsuzawa-Nagata N, et al. Clock gene expression in peripheral leucocytes of patients with type 2 diabetes. *Diabetologia.* 2009;52:329–335.
7. Gekakis N, Staknis D, Nguyen HB, et al. Role of the CLOCK protein in the mammalian circadian mechanism. *Science.* 1998;280:1564–1569.
8. Bunger MK, Wilsbacher LD, Moran SM, et al. Mop3 is an essential component of the master circadian pacemaker in mammals. *Cell.* 2000;103:1009–1017.
9. Kume K, Zylka MJ, Sriram S, et al. mCRY1 and mCRY2 are essential components of the negative limb of the circadian clock feedback loop. *Cell.* 1999;98:193–205.
10. Okamura H, Miyake S, Sumi Y, et al. Photic induction of mPer1 and mPer2 in cry-deficient mice lacking a biological clock. *Science.* 1999;286:2531–2534.
11. Vitaterna MH, Selby CP, Todo T, et al. Differential regulation of mammalian period genes and circadian rhythmicity by cryptochromes 1 and 2. *Proc Natl Acad Sci U S A.* 1999;96:12114–12119.
12. Turek FW, Joshu C, Kohsaka A, et al. Obesity and metabolic syndrome in circadian Clock mutant mice. *Science.* 2005;308:1043–1045.
13. Woon PY, Kaisaki PJ, Braganca J, et al. Aryl hydrocarbon receptor nuclear translocator-like (BMAL1) is associated with susceptibility to hypertension and type 2 diabetes. *Proc Natl Acad Sci U S A.* 2007; 104:14412–14417.
14. Scott EM, Carter AM, Grant PJ. Association between polymorphisms in the Clock gene, obesity and the metabolic syndrome in man. *Int J Obes (Lond).* 2008;32:658–662.
15. Sookoian S, Gemma C, Gianotti TF, Burgueno A, Castano G, Pirola CJ. Genetic variants of Clock transcription factor are associated with individual susceptibility to obesity. *Am J Clin Nutr.* 2008;87:1606–1615.
16. Fu L, Pelicano H, Liu J, Huang P, Lee C. The circadian gene Period2 plays an important role in tumor suppression and DNA damage response in vivo. *Cell.* 2002;111:41–50.
17. Lin YC, Hsiao TJ, Chen PC. Persistent rotating shift-work exposure accelerates development of metabolic syndrome among middle-aged female employees: a five-year follow-up. *Chronobiol Int.* 2009;26: 740–755.
18. Karlsson B, Knutsson A, Lindahl B. Is there an association between shift work and having a metabolic syndrome? Results from a population based study of 27,485 people. *Occup Environ Med.* 2001;58: 747–752.
19. Suwazono Y, Dochi M, Sakata K, et al. A longitudinal study on the effect of shift work on weight gain in male Japanese workers. *Obesity (Silver Spring).* 2008;16:1887–1893.
20. Hansen J. Risk of breast cancer after night- and shift work: current evidence and ongoing studies in Denmark. *Cancer Causes Control.* 2006;17:531–537.
21. Hofman MA. The human circadian clock and aging. *Chronobiol Int.* 2000;17:245–259.
22. Kunieda T, Minamino T, Katsuno T, et al. Cellular senescence impairs circadian expression of clock genes in vitro and in vivo. *Circ Res.* 2006;98:532–539.
23. Touitou Y, Haus E. Alterations with aging of the endocrine and neuroendocrine circadian system in humans. *Chronobiol Int.* 2000;17: 369–390.
24. Balsalobre A, Brown SA, Marcacci L, et al. Resetting of circadian time in peripheral tissues by glucocorticoid signaling. *Science.* 2000; 289:2344–2347.
25. Kunieda T, Minamino T, Miura K, et al. Reduced nitric oxide causes age-associated impairment of circadian rhythmicity. *Circ Res.* 2008; 102:607–614.
26. Weinert D. Age-dependent changes of the circadian system. *Chronobiol Int.* 2000;17:261–283.
27. Ando H, Yanagihara H, Hayashi Y, et al. Rhythmic messenger ribonucleic acid expression of clock genes and adipocytokines in mouse visceral adipose tissue. *Endocrinology.* 2005;146:5631–5636.
28. Hirota T, Okano T, Kokame K, Shirotani-Ikejima H, Miyata T, Fukada Y. Glucose down-regulates Per1 and Per2 mRNA levels and induces circadian gene expression in cultured Rat-1 fibroblasts. *J Biol Chem.* 2002;277:44244–44251.
29. Cavadini G, Petrzilka S, Kohler P, et al. TNF-alpha suppresses the expression of clock genes by interfering with E-box-mediated transcription. *Proc Natl Acad Sci U S A.* 2007;104:12843–12848.
30. Nonaka H, Emoto N, Ikeda K, et al. Angiotensin II induces circadian gene expression of clock genes in cultured vascular smooth muscle cells. *Circulation.* 2001;104:1746–1748.
31. Mutch DM, Clement K. Unraveling the genetics of human obesity. *PLoS Genet.* 2006;2:e188.
32. James FO, Boivin DB, Charbonneau S, Belanger V, Cermakian N. Expression of clock genes in human peripheral blood mononuclear cells throughout the sleep/wake and circadian cycles. *Chronobiol Int.* 2007;24:1009–1034.
33. Archer SN, Viola AU, Kyriakopoulou V, von Schantz M, Dijk DJ. Inter-individual differences in habitual sleep timing and entrained phase of endogenous circadian rhythms of BMAL1, PER2 and PER3 mRNA in human leukocytes. *Sleep.* 2008;31:608–617.
34. Takimoto M, Hamada A, Tomoda A, et al. Daily expression of clock genes in whole blood cells in healthy subjects and a patient with circadian rhythm sleep disorder. *Am J Physiol Regul Integr Comp Physiol.* 2005;289:R1273–R1279.
35. Burioka N, Koyanagi S, Endo M, et al. Clock gene dysfunction in patients with obstructive sleep apnoea syndrome. *Eur Respir J.* 2008; 32:105–112.
36. Ando H, Ushijima K, Kumazaki M, et al. Associations of metabolic parameters and ethanol consumption with messenger RNA expression of clock genes in healthy men. *Chronobiol Int.* In press.
37. Gomez-Abellan P, Hernandez-Morante JJ, Lujan JA, Madrid JA, Garaulet M. Clock genes are implicated in the human metabolic syndrome. *Int J Obes (Lond).* 2008;32:121–128.

Received June 9, 2009
Accepted September 30, 2009
Decision Editor: Huber R. Warner, PhD

Available online at www.sciencedirect.com
ScienceDirect
Metabolism Clinical and Experimental 58 (2009) 456–459
Metabolism
Clinical and Experimental
www.metabolismjournal.com

Middle-aged Japanese women are resistant to obesity-related metabolic abnormalities

Masaru Sakurai[a,b], Toshinari Takamura[a,*], Katsuyuki Miura[c], Shuichi Kaneko[a], Hideaki Nakagawa[b]

[a]*Department of Disease Control and Homeostasis, Kanazawa University Graduate School of Medical Science, Kanazawa, Ishikawa 920-8641, Japan*
[b]*Department of Epidemiology and Public Health, Kanazawa Medical University, Ishikawa 920-0293, Japan*
[c]*Department of Health Science, Shiga University of Medical Science, Otsu 520-2192, Japan*

Received 24 July 2007; accepted 4 November 2008

Abstract

We attempted to determine sex differences in obesity-related metabolic abnormalities in a relatively large middle-aged Japanese population. The study population consisted of 2935 men and 1622 women who were 35 to 59 years old. Metabolic abnormalities were determined using the Japanese criteria for metabolic syndrome, and we evaluated the number of metabolic abnormalities discriminated by waist circumference. In men, the mean number of metabolic abnormalities increased as the waist circumference increased. In women, although the mean number of metabolic abnormalities increased as the waist circumference increased, the mean number was less than 1 even in those with a waist circumference of at least 95 cm. According to the receiver operating characteristic curve, the cutoff levels yielding the maximal sensitivity plus specificity for predicting the prevalence of one or more obesity-related metabolic abnormalities were 80 cm in men and 73 cm in women. However, the positive predictive value was as low as 28.8% in men and 7.1% in women, which may not be suitable for a screening test, especially in women. Middle-aged Japanese women seem to be resistant to obesity-induced metabolic abnormalities, and waist circumference would not effectively predict the existence of metabolic syndrome. In setting the cutoff points in guidelines, a greater emphasis should be placed on the absolute risk of having abnormalities or diseases.

1. Introduction

Cutoff points for waist circumference have been proposed for each racial/ethnic group in diagnosing abdominal obesity and metabolic syndrome [1]. However, the Japanese cutoff points for waist circumference are still controversial. The Japanese cutoff points proposed by the Japan Society of Study for Obesity were derived from a 100-cm^2 area for visceral fat at the umbilical level on computed tomography imaging and are unique in that the value for women (90 cm) is larger than that for men (85 cm) [2,3]. On the other hand, the International Diabetes Federation proposes to use the cutoff point of waist circumference of 90 cm for men and 80 cm for women [1]; and some reports proposed lowering the cutoff point of waist circumference for Japanese women [4,5]. However, previous reports did not pay attention to the absolute risk of the accumulation of metabolic abnormalities in Japanese women. We attempted to determine sex differences in the accumulation of metabolic abnormalities in relation to obesity in a relatively large-scale middle-aged Japanese population.

2. Research design and methods

The study population consisted of 4557 Japanese employees (2935 men and 1622 women) of a metal products factory who were aged 35 to 59 years. Detailed information on this study population has been provided elsewhere [6,7]. The physical examinations for this analysis were held in 1996. Anthropometric markers including waist circumference and blood pressure were measured, and venous blood samples after an overnight fast were withdrawn from each subject during a routine annual medical checkup. Three obesity-related abnormalities—high blood

* Corresponding author. Tel.: +81 76 265 2234; fax: +81 76 234 4250.
E-mail address: ttakamura@m-kanazawa.jp (T. Takamura).

0026-0495/$ – see front matter © 2009 Elsevier Inc. All rights reserved.
doi:10.1016/j.metabol.2008.11.001

pressure, dyslipidemia, and high fasting plasma glucose—were defined by the Japanese guidelines of metabolic syndrome [3]. *High blood pressure* was defined as a systolic blood pressure of at least 130 mm Hg or a diastolic blood pressure of at least 85 mm Hg. *Dyslipidemia* was defined as serum triglycerides of at least 150 mg/dL or high-density lipoprotein cholesterol not exceeding 40 mg/dL, and *high fasting plasma glucose* was defined as a fasting plasma glucose of at least 110 mg/dL. We evaluated the number of obesity-related abnormalities discriminated by waist circumference and body mass index (BMI). We plotted receiver operating characteristic (ROC) curves for waist circumference to predict one or more obesity-related metabolic abnormalities and calculated sensitivity, specificity, and positive predictive value.

3. Results

The participants had a mean age of 45.5 years for men and 45.3 years for women, a mean BMI of 23.3 kg/m^2 for men and 22.6 kg/m^2 for women, and a mean waist circumference of 80.1 cm for men and 72.7 cm for women.

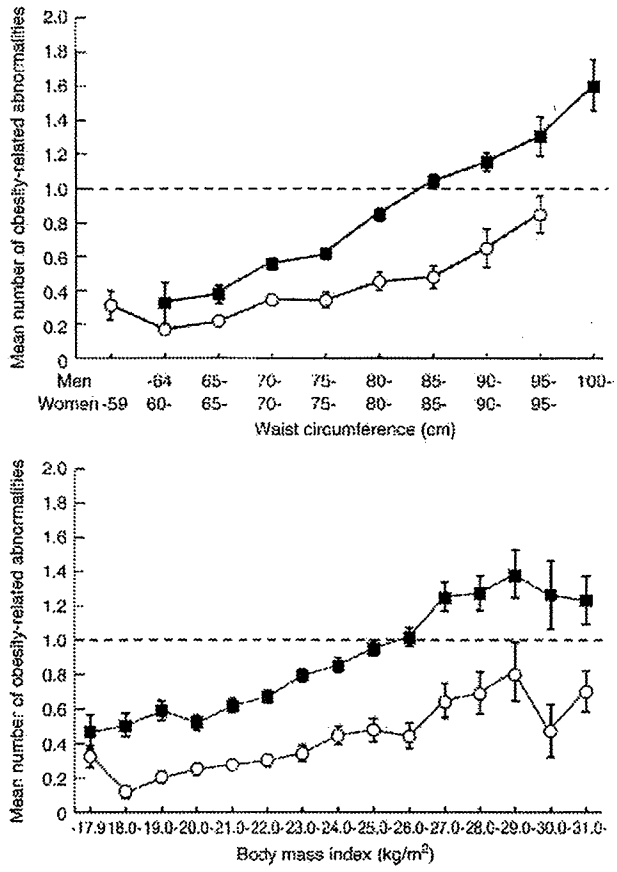

Fig. 1. The mean number of obesity-related abnormalities discriminated by waist circumference or BMI in men (■) and women (○). Obesity-related abnormalities included hypertension, dyslipidemia, and glucose intolerance. The horizontal dotted line shows a mean number of obesity-related abnormalities of 1.0. Data are presented as means ± standard error.

We evaluated the association between waist circumference or BMI and the mean number of obesity-related abnormalities (Fig. 1). In men, the mean number of abnormalities increased as waist circumference or BMI increased. When the waist circumference was 85 cm, which is the cutoff point for the diagnosis of metabolic syndrome in Japanese men [3], the mean number of complicated metabolic abnormalities was approximately 1. In women, although the mean number of abnormalities increased as the waist circumference increased, it was less than 1 even in women with a waist circumference of at least 95 cm or BMI of at least 30 kg/m^2.

The prevalence of one or more obesity-related abnormalities was 50% in men and 21% in women. According to the ROC curve, the area under the curve was higher for men (0.675; 95% confidence interval, 0.655-0.694) than for women (0.627; 95% confidence interval, 0.596-0.657) (Fig. 2). The cutoff levels yielding the maximal sensitivity plus specificity for predicting the prevalence of one or more obesity-related abnormalities were 80 cm in men (sensitivity, 0.59; specificity, 0.69) and 73 cm in women (sensitivity, 0.55; specificity, 0.64). However, the positive predictive value was as low as 28.8% in men and 7.1% in women at these cutoff points.

4. Discussion

Hara et al [4] and Ohkubo et al [5] proposed a cutoff point regarding waist circumference for detecting metabolic syndrome or insulin resistance in Japanese based on relatively small, older, and somewhat higher-risk populations. Both reports proposed lowering the cutoff point of waist circumference for Japanese women to 76 cm. We found that a similar cutoff point of 73 cm for women provided the highest sensitivity and specificity for detecting metabolic syndrome as was recently observed [4,5]. Theoretically, sensitivity and specificity (therefore, the ROC curves) are not affected by the prevalence of the detected disease in various populations. However, the positive predictive value was as low as 7.1% in our population of middle-aged Japanese women, which means that only 7.1% of women with waist circumference of 73 cm or higher had the accumulation of metabolic abnormalities. Therefore, this cutoff point may not be suitable for a screening test in women. Two previous reports from Japan did not give the positive predictive values for their cutoff points. The low positive predictive value was caused by the low prevalence of metabolic abnormalities in middle-aged Japanese women and, possibly, the relatively higher resistance of Japanese women than men to obesity-induced metabolic abnormalities. As proposed in previous reports [4,5], lower cutoff points for

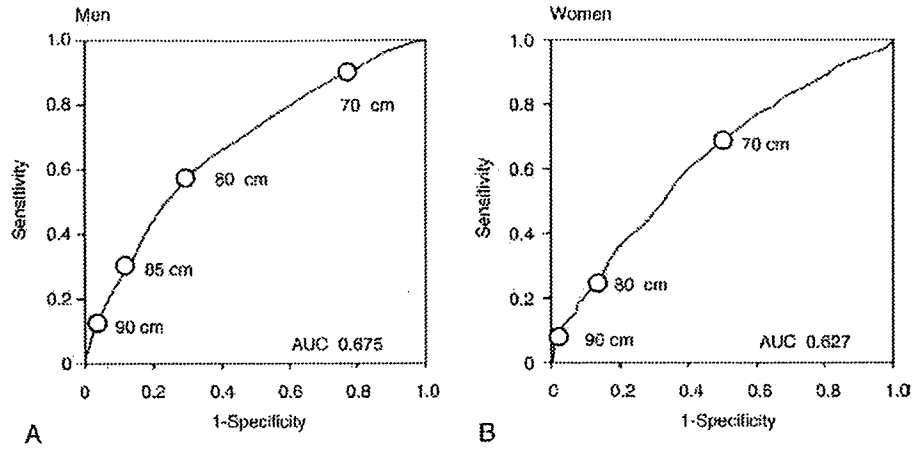

Cutoff point for waist circumference

	Sensitivity	Specificity
Men		
70 cm	0.94	0.16
80 cm	0.59	0.69
85 cm	0.32	0.86
90 cm	0.13	0.96
Women		
70 cm	0.67	0.52
73 cm	0.55	0.64
80 cm	0.27	0.85
90 cm	0.09	0.98

C

Fig. 2. The predictive performance of waist circumference for one or more obesity-related metabolic abnormalities. The ROC curves for one or more obesity-related metabolic abnormalities in men (A) and in women (B) are shown. The sensitivity and specificity of each cutoff point of waist circumference are given (C).

waist circumference might detect more people with metabolic abnormalities with high sensitivity. However, in a population with a low prevalence of metabolic abnormalities, lower cutoff points would also result in a greater proportion of false positives, with more healthy women in particular being screened as abnormal. Furthermore, because the mean number of complicated metabolic abnormalities was lower than 1 even in those with a waist circumference of at least 95 cm and the area under the ROC curve was lower in women than in men, waist circumference would not effectively predict the existence of metabolic syndrome in Japanese women.

In this study, similar to previous reports [2,4,5,8], cutoff points of waist circumference were proposed using ROC curves for predicting the metabolic abnormalities. However, abdominal obesity is important in metabolic syndrome because it has been linked to the development of cardiovascular disease. Further investigations are needed to evaluate the association between waist circumference and future incidence of cardiovascular events to establish an appropriate cutoff point for waist circumference. Another limitation was that the participants of this study did not include older people and might be healthier than general Japanese people because they were identified at a work place. Similar analyses are needed in older Asian populations.

In conclusion, middle-aged Japanese women seem to be resistant to obesity-related metabolic abnormalities; and waist circumference would not effectively predict the existence of metabolic syndrome. In setting cutoff points in guidelines, a greater emphasis should be placed on the absolute risk of having abnormalities or diseases.

References

[1] Arberti KG, Zimmet P, Shaw J, for the IDF Epidemiology Task Force Consensus Group. The metabolic syndrome—a new worldwide definition. Lancet 2005;366:1059-62.
[2] The Examination Committee of Criteria for "Obesity Disease" in Japan, Japan Society for Study of Obesity. New criteria for 'obesity disease' in Japan. Circ J 2002;66:987-92.
[3] Oda E, Watanabe K. Japanese criteria of metabolic syndrome. Circ J 2006;70:364.
[4] Hara K, Matsushita Y, Horikoshi M, Yoshiike N, Yokoyama T, Tanaka H, et al. A proposal for the cutoff point of waist circumference for the diagnosis of metabolic syndrome in the Japanese population. Diabetes Care 2006;29:1123-4.
[5] Ohkubo T, Kikuya M, Asayama K. A proposal for the cutoff point of waist circumference for the diagnosis of metabolic syndrome in the Japanese population. Diabetes Care 2006;29:1986-7.

[6] Sakurai M, Miura K, Takamura T, Ota T, Ishizaki M, Morikawa Y, et al. Gender differences in the association between anthropometric indices of obesity and blood pressure in Japanese. Hypertens Res 2006;29:75-80.

[7] Morikawa Y, Nakagawa H, Ishizaki M, Tabata M, Nishijo M, Miura K, et al. Ten-year follow-up study on the relation between the development of non–insulin dependent diabetes mellitus and occupation. Am J Ind Med 1997;31:80-4.

[8] Ko GT, Chan JC, Cockram CS, Woo J. Prediction of hypertension, diabetes, dyslipidaemia or albuminuria using simple anthropometric indexes in Hong Kong Chinese. Int J Obes Relat Metab Disord 1999;23: 1136-42.